Instability and Transition of Flow at, and Near, an Attachment-Line - Including Control by Surface Suction

Contract Number NCC1-218

A Smith
D I A Poll

Flow Control and Prediction
Cranfield College of Aeronautics
Cranfield University
Bedford
UK

Summary

Experiments have been performed on an untapered, swept cylinder model in the Cranfield College of Aeronautics 8'x6' low speed wind tunnel to investigate the effect of surface transpiration on the process of relaminarisation in the attachment-line boundary layer.

Values of the characteristic Reynolds number, $\overline{R}$, up to 1000 were investigated and it was found that a turbulent attachment-line flow could be relaminarised using modest suction rates ($C_q \approx -0.003$), even when suction is applied over areas with relatively small streamwise extent (between 265 and 410 boundary layer thicknesses). Suction coefficients for complete suppression of turbulence were determined as a function of $\overline{R}$ and s/η.

Using suction levels of up to -5% of the freestream flowrate no evidence of the relaminarised flow reverting to the turbulent state, ie transition through oversuction, was found for the surface under consideration.

When a relaminarised attachment-line encounters a non-porous surface it was found that the subsequent retransition occurred under the same conditions as natural transition, ie the relaminarised boundary layer behaves as though it had always been laminar.

The effect of attachment-line suction on the spanwise propagation of gross disturbances emanating from the fuselage-wing junction region was also studied. It was found that, for the limited conditions that could be studied with this model-tunnel combination, complete relaminarisation could not be obtained for the suction levels available over the relatively short spanwise distance ($s/\eta \approx 2500$) from the junction. Turbulent flow could be partially relaminarised, with the intermittency reduced to about 30%. However, full relaminarisation should be obtained with either increased suction on the attachment-line, the addition of suction on the fuselage upstream of the junction, or the use of a longer spanwise length of suction surface.

Finally, the effect of blowing on a laminar attachment-line boundary layer was also considered, and excellent agreement was achieved with previous work by Danks *et al*, and the theoretical work of Theofilis.

Contents

List of Figures

Notation

α_i	spatial amplification rate, from linear stability theory
η	viscous length scale (m)
ν	kinematic viscosity (m^2 /s)
ρ	density (kg/m^3)
A	Ellis oversuction parameter
C	chord (m)
C_q	suction coefficient
d_h	hole diameter (m)
D	model diameter (m)
f	frequency (Hz)
F	non-dimensional stability theory frequency (10^6 2π f ν/V_e^2)
p_a	attachment line static pressure (N/m^2)
p_s	static pressure (N/m^2)
q	dynamic pressure (N/m^2)
Q	freestream velocity (m/s)
$\overline{Q}$	empty tunnel freestream velocity (m/s)
$\overline{R}$	leading edge Reynolds number
$R_{\theta lam}$	attachment-line transition Reynolds number based on laminar momentum thickness
s	general spanwise distance (m)

s_{TT} spanwise distance from the start of the suction surface (mm)
U chordwise velocity (m/s)
v_o^* suction parameter used by Pfenninger; equivalent to $\overline{R}\, C_q$
V spanwise velocity (m/s)
V_h transpiration surface hole velocity (m/s)
w(0) suction velocity perpendicular to suction surface (m/s)
w_h flow speed through suction hole (m/s)
x chordwise distance (m)

Subscripts

∞ freestream conditions

1. Introduction

Advances in aviation during and following the Second World War led to an enormous improvement in the performance of aircraft. The push for enhanced efficiency brought cruise speeds into the transonic range, where the associated drag rise due to the appearance of shock-waves became a limiting factor. Wing sweep was adopted to delay the onset of this drag rise, but with this development came several new and unforeseen problems.

Preliminary theoretical work assumed that the boundary layer transition characteristics of a swept wing would be subject to the independence principle, so the chordwise transition position could be predicted from two-dimensional work. However, during flight tests on swept wing aircraft by Gray in 1952[1], transition due to cross-flow instability, with its characteristic 'saw-tooth' transition front, was discovered. He also found that as sweep angles increased beyond 20° the transition front moved swiftly towards the leading edge and, at larger sweep angles, transition occurred at the leading edge itself. Attachment-line contamination was also observed, but was not identified as an independent mechanism. Cross flow instability was demonstrated theoretically by Owen and Randall[2] and Squire in the same year. Ten years later, laminar flow projects were launched by Northrop and Handley Page incorporating wing sections designed to avoid cross-flow instability. During flight tests it was found that transition occurred close to the leading edge and very little laminar flow was obtained. Investigations were started in the early 1960's, by Pfenninger at Northrop and Gaster at Cranfield, to find the cause of this premature transition. Attachment-line transition was identified as an independent mechanism and several ideas were proposed for its control. However, interest in laminar flow had waned and funding for the research was stopped. Following the oil crisis of the early 1970's, interest in leading edge flows resumed in the mid-1970's with a number of initiatives, including the NASA Space Shuttle and Aircraft Energy Efficiency/Laminar Flow Control (ACEE/LFC) research programs.

Gas turbine development has now reached a point where additional increases in efficiency are both difficult and expensive to achieve. Consequently, aircraft manufacturers are looking elsewhere for ways to reduce Direct Operating Costs (DOC's) or increase military performance. The attention of industry is currently focusing on hybrid laminar flow control (HLFC) as a possible method of reducing DOC's for civil aircraft. The combination of a natural laminar flow aerofoil and active flow control at the leading edge can produce laminar flow over 50-60% of upper surface chord, leading to a reduction in total aircraft drag of up to 15%[3]. By further extending the use of laminar flow control to tail-fins, engine nacelles and pylons the potential reduction in drag becomes very significant.

Previous work by Danks and Poll[4], carried out under Contract Number NAGW-3871, considered the transition process at, and near, an infinite swept attachment-line, with particular emphasis on cross-flow instability. Using a large scale, suction cylinder several problems were examined: the time-dependent signals and spectra describing flows subjected to large cross-flow induced instabilities, the effect of attachment-line transpiration on cross-flow transition, the suction distributions which produced transition at a fixed chordwise location for a fixed sweep angle, the effect of transpiration on stability and transition at the attachment-line, the possible link between attachment-line disturbance frequencies and the frequency of vortex shedding at the

trailing edge, and the propagation of gross disturbances through the attachment-line flow in the immediate vicinity of a wing-fuselage junction.

Following this study and discussions with NASA Langley and Boeing a different series of questions have been addressed in the present work. There are five areas of interest :

- Relaminarisation of the attachment-line boundary layer when the value of $\overline{R}$ exceeds 600
- The effects of large suction levels on transition in the attachment-line boundary layer (ie critical oversuction)
- The transition characteristics of a relaminarised attachment-line flow which encounters a non-porous surface
- The effect of attachment-line suction on the spanwise propagation of gross disturbances emanating from the wing-fuselage junction
- The attachment-line transition caused by surface blowing.

2. The Swept Wing Boundary Layer

2.1 General Swept Conditions

As an aircraft's speed increases the freestream Mach number increases and eventually, at some particular point on the wing surface, the flow speed will reach Mach one. At still higher speeds a small region of supersonic flow is established which is terminated by a shock wave. Shock wave/boundary layer interactions cause a large increase in drag and may produce shock-stall if the adverse pressure gradient behind the shock wave causes the boundary layer to separate. The onset of the drag rise can be delayed to higher flight speeds by sweeping the wing and this is the most common technique currently employed.

2.2 The Attachment-Line and Infinite Swept Conditions

An important consequence of wing sweep is the creation of an attachment-line flow. Referring to the wind axis system the freestream can be split into two components; the chordwise flow and a spanwise flow. The attachment line is defined as the line along the leading edge which separates the flow over the upper surface from that over the lower surface. The streamline pattern around a swept leading edge is shown in Figure 1, with the attachment-line indicated by the line A-A. It can be seen that the flow close to the attachment-line is highly three-dimensional, characterised by curved streamlines. The condition of the attachment-line has an important effect on the state of the downstream chordwise boundary layer, since fluid from the attachment line remains within the wing boundary-layer.

To simplify study of the physics of attachment-line flow it is convenient to reduce the number of independent variables by aiming for infinite swept conditions. A model with constant spanwise geometry can be used to produce an attachment-line boundary layer with spanwise independent properties (e.g. boundary layer thickness, skin friction, the rate of divergence, etc.) provided the boundary layer is either laminar or turbulent, but not transitional[5]. The spanwise independence is achieved by the transfer of fluid from the attachment-line into the chordwise boundary layer. This is just balanced by the entrainment of fluid from the freestream into the attachment-line boundary layer.

2.3 Cross-Flow Instability

All three-dimensional boundary layers are characterised by streamline curvature. This is maintained by a pressure gradient that acts perpendicular to the external streamline direction in a plane drawn parallel to the surface. Fluid is slowed by

viscosity in the boundary layer and moves in the direction of this gradient to create a "cross-flow" velocity component. For the cross-flow component of the profile the boundary conditions are no slip at the surface and zero velocity at the edge of the boundary layer. It follows that such a profile contains at least one point of inflection and consequently indicates that, as demonstrated by Gregory *et al*[6], such profiles first become unstable at very low Reynolds numbers.

2.4 Intermittency

When a boundary layer is transitional, flow parameters at a fixed measuring station are found to switch almost instantaneously between the laminar and turbulent states. This characteristic was used by Emmons[7] to define intermittency, Γ, being the probability that, at a particular time, t, the flow at a given location is turbulent. Therefore, for purely laminar flow the intermittency is zero and for fully turbulent flow the intermittency is unity.

2.5 Parameters Used for The Study of Attachment-Line Flows

The flow field at the leading edge of an aircraft wing is governed by many parameters and restrictions need to be applied to the experimental system to reduce the problem to manageable proportions. A simple approach is the use of a model with constant spanwise section to give infinite swept conditions. The effects of compressibility can be ignored if the spanwise Mach number at the edge of the attachment-line boundary layer is less than 0.2.

With these constraints, steady, incompressible flow without heat transfer, along an infinite-swept attachment line is completely determined by the magnitude of the characteristic Reynolds number, $\overline{R}$. By analogy with the Blasius length scale a suitable viscous length scale is,

$$\eta = \left[\frac{\nu}{dU_e / dx} \right]_{x=0}^{\frac{1}{2}}$$

This is approximately equal to the displacement thickness when there is no surface transpiration.

The natural leading edge Reynolds number, $\overline{R}$, is therefore

$$\overline{R} = \frac{V_e \eta}{\nu_e}$$

This can be related to other characteristic Reynolds numbers used in the study of leading edge flows by

$$R_{\delta^*} = 1.026\overline{R}$$

$$R_{\theta} = 0.404\overline{R}$$

When the attachment-line behaviour is investigated at different spanwise positions a length parameter s is introduced, where s is the spanwise distance under consideration (eg the spanwise length between the position of a trip wire and the measuring station or the spanwise length between the end of the suction surface and the measuring station). The associated non-dimensional group is then,

$$\frac{s}{\eta}$$

When surface transpiration is used a further parameter is required; this may take the form of a transpiration coefficient:

$$C_q = \frac{w(0)}{V_e}$$

A positive transpiration coefficient represents blowing and a negative coefficient suction.
It follows that measurements made at any point along the leading edge and at any sweep angle can be compared provided that the three non-dimensional parameters $\overline{R}$, s/η, and C_q are duplicated.

3. The Model

Tests have been conducted on a large swept cylinder model. This has a circular leading edge, faired to a "tear drop" section to prevent early separation and the possible formation of an oscillating wake. The spanwise chord is 0.813m and the leading edge radius is 0.203m. A perforated surface is made from 1.2mm thick titanium sheet laser drilled, prior to model construction, with holes of 50μm diameter and hole-to-hole and row-to-row spacing of 400μm, shown in Figure 2. The entire drilling pattern is skewed relative to the axis of symmetry by 14°, leading to a streamwise hole separation of not less than 1600μm and in general an irregular streamwise pattern of holes.

The titanium surface is divided into perforated and non-perforated areas to enable a range of suction conditions and distributions to be considered. A plan of the perforated areas is given as Figure 3. The regions of perforated surface are further divided into areas supplied by independent plenum chambers, shown in .Figure 4, which permit the use of distributed suction. For the current investigation, transpiration at the attachment-line was provided by a region which begins 1.35m from the upstream tip and

extends 0.9m along the leading edge. This extends ±10° either side of the attachment line and is served by a single plenum chamber. The plenum is connected via valves and flowmeters to a vacuum tank which has a maximum suction capacity of approximately 3000 litres/minute. The model was mounted in the Cranfield College of Aeronautics low-speed, closed-return, wind tunnel which has a 2.44m x 1.83m working section and a maximum freestream velocity of 55m/s.

4. The Estimation of Flow Parameters

The accurate determination of the leading edge Reynolds number is of critical importance. However, in previous investigations (eg Pfenninger[8] and Gaster[9]) the accuracy was compromised by two issues: (i) the use of an empirical blockage correction to calculate the freestream velocity and, hence, the attachment-line velocity and (ii) the use of the geometric (measured) sweep angle. The method used in these experiments involves neither the use of a blockage correction nor the measurement of sweep angle (except in approximate terms for reference).

At low freestream Mach numbers, the effects of compressibility can be neglected and Bernoulli's equation is accurate. Knowing the empty tunnel calibration (ie the relation between the static pressure difference across the contraction cone and the working section dynamic pressure with no model in place) and the static pressure at the start of the working section, the freestream total pressure is known. Hence, by measuring the static pressure on the attachment-line, the local dynamic pressure along the attachment line can be deduced (assuming infinite swept conditions) and, hence, the attachment-line edge velocity, V_e.

$$V_e = \left[\frac{(q + p_s)_\infty - p_a}{\frac{1}{2}\rho_\infty} \right]^{\frac{1}{2}}$$

The arrangement of the model in the working section is shown in Figure 5. It was aligned in the working section using the static pressure distribution around the leading edge of the model as a yaw meter. If the model is correctly aligned the static pressure coefficient distribution at any spanwise point should be symmetric about the attachment-line. Figure 6 shows a typical aligned and untwisted distribution. By comparing the pressure distributions around the top, middle, and bottom of the leading edge any yawing or twisting of the model is apparent and the alignment with the freestream can be set accurately.

Once the model has been aligned the chordwise velocity gradient at the attachment-line, $(dU_e/dx)_{x=0}$, can be found from the same static pressure distributions. There are two sets of static tappings on the model (440mm and 2260mm from the upstream tip), each extending to 85° either side of the line of geometric symmetry in steps of 5°. A sample distribution is shown in Figure 6.

From Bernoulli's equation, the attachment-line static pressure and the static pressure at any chordwise position are related by,

$$p_a - p_s = \frac{1}{2}\rho U_e^2$$

Hence, the chordwise velocity distribution around the leading edge of the model can be calculated. The chordwise velocity is non-dimensionalised using the empty tunnel freestream velocity, $\overline{Q}_\infty$, and the chordwise surface distance using the chord, C. The empty tunnel freestream velocity is used because this can be determined accurately from the empty tunnel calibration. In the region near to the attachment-line the relationship between $U_e/\overline{Q}_\infty$ and x/C is linear and the gradient can be determined by a least-squares approximation. The chordwise velocity gradient is therefore,

$$\left[\frac{dU_e}{dx}\right]_{x=0} = \left[\frac{d\left(U_e/\overline{Q}_\infty\right)}{d\left(x/C\right)}\right]_{x=0} \cdot \frac{\overline{Q}_\infty}{C}$$

An example of this method applied to the upstream pressure tappings is shown in Figure 7.

5. Boundary Layer Relaminarisation by Suction When the Attachment-Line Reynolds Number Exceeds 600

5.1 Experimental Method

A 4mm diameter trip wire was wrapped around the leading edge of the model 900mm from the upstream tip. At values of $\overline{R}$ in excess of 600, d/η is greater than 6.5 which, as shown by Poll[10], constitutes a gross trip (ie turbulence is shed directly from the wire and transition occurs at the trip location). Therefore, the attachment-line boundary layer is turbulent and fully developed at the start of the suction region.

A hot-wire probe was placed at the required distance from the start of the suction surface. Care was taken to ensure that the wire was as close to the model surface as possible. The highly reflective surface finish of the titanium sheet was useful in this regard since the spacing between the surface and the hot wire probe could be reduced until the probe and its mirror image almost touched. Using this method the probe height could be reliably set closer than 0.5mm.

To take a data point, the freestream dynamic pressure was set and the suction rate was varied until the hot-wire signal indicated that relaminarisation had occurred. The suction rate was then noted.

5.1.1 Relaminarisation Criterion

Relaminarisation was judged to have occurred when, at constant working section dynamic pressure, just two or three turbulent bursts occurred every two seconds. This situation can be repeated reliably and with good accuracy. It should be noted that, by contrast, the condition at which all turbulent bursts are extinguished is very difficult to determine, as is the condition when the flow is completely turbulent ie the end of transition.

5.2 Duplication of Previous Work

The work performed previously by Danks and Poll [4] was conducted using the same model mounted in the 9' x 7' low-speed wind-tunnel in the Goldstein Laboratory at the University of Manchester. As a result of this change of wind tunnel environment, it was necessary for some of the work to be repeated. It was decided to repeat the cases with a sweep angle of 60°, giving $\overline{R}$ values up to 550, and with the hot-wire placed 700mm downstream from the beginning of the suction surface (2050mm from the upstream tip).

5.2.1 Preliminary Results

At the beginning of the programme, the operator (Smith) was unfamiliar with the method used here to identify relaminarisation but with help from Dr Danks (an experienced operator), his ability improved rapidly. This was apparent in the way that, over repeated attempts, the suction rates judged to cause relaminarisation for identical conditions decreased. This is shown in Figure 8. It demonstrates both the difficulty of the experimental technique and how easy it is for an inexperienced operator to use excess suction.

The final results are given as Figure 9. The agreement with Danks and Poll's previous data is good (well within experimental uncertainty) showing that the change of wind tunnel environment has very little effect.

5.3 Presentation of Data

As noted in Section 2, three non-dimensional groups are required to describe the flow conditions at the attachment-line completely. It follows that to compare results obtained under different conditions (eg differing sweep angle) all three non-dimensional parameters must be used. For example, Figure 9 illustrates the duplication of results by different operators in different wind tunnels. Here $\overline{R}$ and C_q are shown at a specific

value of s, without reference to the applicable non-dimensional parameter s/η. In this case this is acceptable because the same physical conditions were being compared (sweep angle and distance s and therefore s/η) but, if different sweep angles had been used for each data set, the s/η values would have been different and plotting the data in this way would have been erroneous.

5.3.1 Data Reduction

In their original work, Danks and Poll found that, as $s/\eta \to \infty$, the effect of s/η diminished and that, for s/η greater then 3000, an asymptotic state was reached. An empirical relation was presented which allowed the effect of s/η to be removed by 'normalisation'. In this way, the suction coefficient results can be corrected to give the value as $s/\eta \to \infty$. A scaling parameter, w', was defined so that the suction coefficient which would be required at the limit of $s/\eta \to \infty$ could be calculated by

$$\left(C_q\right)_{s/\eta\to\infty} = \frac{\left(C_q\right)_{s/\eta<\infty}}{w'}$$

$$w' = 1 + \exp(2.0 - 0.0025\, s/\eta)$$

for $500 < s/\eta < \infty$

Danks and Poll also found that, in the limit as $s/\eta \to \infty$:

$$\overline{R} \approx 245\sqrt{(1.07(C_q\overline{R})^2 - 0.48(C_q\overline{R}) + 1)}$$

for $250 < \overline{R} < 550$

5.4 New Work

Danks and Poll investigated the effects of surface transpiration on the attachment-line boundary layer for values of $\overline{R}$ up to 600. However, in future ultra-large aircraft, the leading edge Reynolds numbers may be as large as 1000 in the cruise condition. With this in mind, work was undertaken to extend the experimental data to $\overline{R}$ values of approximately 1000.

For these tests, a geometric sweep angle of 70° was used, giving a maximum $\overline{R}$ of approximately 1000. The state of the boundary layer was monitored at four locations on the suction surface in turn, using a hot-wire anemometer placed on the attachment-line 495mm, 610mm, 700mm, and 810mm downstream of the start of the suction

surface (1845mm, 1960mm, 2050mm and 2160mm from the upstream tip). In each case, the suction rate required to produce relaminarisation of the boundary layer at a fixed value of $\overline{R}$ was determined.

5.4.1 Results

Bearing in mind the points raised in Section 5.3, Figure 10 shows the effect of increasing s/η on the suction coefficient required to produce relaminarisation, at a fixed value of $\overline{R}$. It can be seen that, as s/η increases, the suction coefficient required to cause relaminarisation, at a given $\overline{R}$, decreases and approaches a constant value asymptotically. From these results and the data from Danks and Poll, the asymptotic value is reached at $s/\eta \geq 2000$. The asymptotic value of the suction coefficients at each $\overline{R}$ can, therefore, be found, and these are given in Table 1.

$\overline{R}$	Asymptotic Suction Coefficient ($x10^3$)
650	-3.4
700	-3.3
750	-3.3
800	-3.3
850	-3.2
900	-3.2
950	-3.2

Table 1 Values of Suction Coefficient Required For Relaminarisation in the Limit as $s/\eta \rightarrow \infty$.

Fitting a curve to these data gives an empirical relation between $\overline{R}$ and C_q, in the limit of $s/\eta \rightarrow \infty$. The relation given in Section 5.3.1, from Danks and Poll, is a curve fitted to their asymptotic suction coefficient data, and a comparison is, therefore, possible, see Figure 11. The Danks and Poll relation was obtained from results for $250 < \overline{R} < 550$, and they predicted that, at large $\overline{R}$, a suction coefficient existed at which it was impossible for the boundary layer to be turbulent, irrespective of $\overline{R}$. The C_q value given was -0.0035 and the Danks and Poll relation has been extrapolated to show this. The asymptotic suction coefficients obtained in the current experiments are lower than the values predicted by Danks and Poll, showing a suction coefficient of approximately -0.0033 for turbulent flow to be impossible. The difference is not entirely surprising, because the values of $\overline{R}$ used in this work were almost double those used by Danks and Poll.

The w' values for the current data were evaluated and are compared with the Danks and Poll relation in Figure 12. The scatter of the Danks and Poll data is shown by error bars.

The data show good agreement except at small s/η , where the effects of s/η are very large.

5.5 Conclusions

Experiments performed at Manchester have been duplicated successfully at Cranfield. The conditions for relaminarisation of a turbulent attachment-line boundary layer using suction have been extended to $\overline{R}$'s of approximately 1000. The trends seen in previous work have been reproduced, and the data now cover a range of $\overline{R}$'s that comfortably exceeds the flight conditions of current large transport aircraft.

In the limit of $s/\eta \rightarrow \infty$, the suction coefficient required to relaminarise a turbulent attachment-line boundary layer approaches an asymptotic a value of approximately -3.3×10^{-3} at which turbulent attachment-line flow is not possible, at any value of $\overline{R}$.

6. The Effects of Large Suction Levels on Transition in the Attachment-Line Boundary Layer

During the last fifteen years, laminar flow control has moved from research to industrial application. This has raised the question of what would happen if the suction system failed. The use of very large suction amounts is considered in this Section and the reversal of the flow direction (ie blowing rather than suction) is addressed in Section 7.

The effect of large suction levels on a two-dimensional, flat plate boundary layer has been studied previously [11], where it was found that, at sufficiently high suction coefficients, transition could occur at a lower Reynolds number than if no suction had been used. This is termed Critical Oversuction. This definition is quite specific: only when the suction transition Reynolds number is lower than the Reynolds number at which transition would have occurred without the use of suction can it be said that critical oversuction has occurred. When suction is applied, each of the holes in the porous surface becomes a sink and the sink effect causes the formation of a 'horse-shoe' vortex around the hole, which introduces a perturbation into the boundary layer. With sufficiently large suction coefficients, the combination of the effects of all the holes can produce a disturbance that causes transition to occur prematurely.

Running concurrently with the relaminarisation experiments, tests were made to investigate the issue of critical oversuction. At each of the spanwise positions used in the relaminarisation tests, the largest suction rates possible were used. Measurements were made at values of $\overline{R}$ ranging from 156 to 954, and with suction coefficients ranging from -0.100 to -0.004. The maximum suction rate was limited by the experimental apparatus (at approximately 4000 litres/minute), so the suction coefficient was inversely proportional to the boundary layer edge velocity. Therefore, the largest suction coefficient was obtained at the smallest $\overline{R}$.

No sign of oversuction was found and the attachment-line remained laminar throughout the tests.

6.1 Comparison With Pfenninger Data

The results commonly quoted as evidence for critical oversuction at an attachment-line were produced by Pfenninger[8]. Using a blunt-nosed wing swept at 45°, he experimented with attachment-line transition control using suction through slots and perforations. With strong suction upstream of the test zone the attachment-line boundary layer was relaminarised so that the attachment-line was laminar at the start of the porous test surface. Pfenninger investigated how suction could be used to delay the transition of the laminar boundary layer and the results are given in Figure 13. The suction parameter v_o^* is equivalent to $\overline{R}\, C_q$ using the terminology of this report. From Figure 16 it can be seen that, at large spanwise Reynolds numbers (Wz/ν), as the suction parameter v_o^* increases, the effect of the suction decreases. At high suction rates, the laminar momentum thickness Reynolds number at transition is less than that for medium suction rates. Pfenninger attributed this reduction to the formation of longitudinal disturbance vortices originating from the suction holes and triggering transition (ie critical oversuction). The data has been replotted in terms of $\overline{R}$ and C_q, as Figure 14. This shows that, at each spanwise position, as the suction coefficient is increased the transition $\overline{R}$ increases. At no spanwise position does an increase in the suction coefficient cause a reduction in the transition $\overline{R}$, or cause transition to occur at an $\overline{R}$ lower than that with no suction. According to our definition, Pfenninger did not see critical oversuction and it was the way the data was plotted that gave the impression of an adverse suction effect.

However, replotting the data does raise one important point: as Pfenninger increased the suction, the $\overline{R}$ increased by 23% but the suction coefficient increased by 350%. This is a huge increase, especially considering that Pfenninger was starting with a laminar attachment-line and was simply delaying the transition to turbulence, not relaminarising a turbulent boundary layer. These sort of results are usually encountered when the suction system has a leak, where a disproportionately large increase in suction is required to produce a small increase in performance.

6.1.1 Ellis Criterion

A comprehensive experimental study of the problem in two-dimensional flow, carried out by Ellis[11], has produced an empirical criterion for critical oversuction conditions,

$$\frac{w_h d_h^2}{V_e \delta^{*2}} = A$$

where A is a constant. From Ellis's work, critical oversuction occurred for two-dimensional (flat plate) flow when A exceeded approximately 2.

Pfenninger's data and the current data were compared with Ellis' criterion and it was found that the largest value of the Ellis parameter from Pfenninger's data was only 0.05, at an $\overline{R}$ of 841, while the current data had an Ellis parameter of 21. This also suggests that Pfenninger did not encounter oversuction.

The largest suction coefficient achieved in the current tests was at an $\overline{R}$ of 156, (a sweep angle of 15°). 3000 litres/min of air were removed from the surface, at a freestream velocity of approximately 7m/s, which gave a suction coefficient of -0.100, at a unit Reynolds number of 1.003×10^6 m^{-1}. This is one hundred times larger than the suction coefficient required to relaminarise a fully turbulent attachment-line.

One difference between this case and Pfenninger's work could be the receptivity of the attachment-line. Pfenninger's tests were conducted at high $\overline{R}$ ($650<\overline{R}<800$), when the attachment-line without suction was linearly unstable, whereas the above example was at $\overline{R}=156$, when the attachment-line was stable without suction. The receptivity of the boundary layer must play a part in the transition process, but the suction coefficients used in the present tests were so large that it seems unlikely that the receptivity was the dominant factor. It should be noted that the relaminarisation data, presented in Section 5, was taken at $560<\overline{R}<960$, which is similar to the range used by Pfenninger, and no retransition was observed up to the highest suction coefficients achievable.

6.2 Conclusions

Critical oversuction was never observed in the present tests, even at a suction coefficient of -0.100.

Comparing the current work with the results of Pfenninger showed that he was using lower suction coefficients, and when his results were analysed using Ellis' parameter it was found that the oversuction parameter was lower than in the current tests. Therefore, we conclude that Pfenninger's data do not provide reliable evidence of critical oversuction.

7. An Investigation of the Transition Which Occurs When a Relaminarised Attachment-Line Encounters a Non-Porous Surface

The results in Section 5 and those shown previously[4] demonstrate that a turbulent attachment-line can be relaminarised using surface suction. Having relaminarised the attachment-line boundary layer, it is necessary to know how the relaminarised flow will behave once it leaves the suction surface and moves onto a non-porous surface.

7.1 Experimental Arrangement

For these tests the model was swept forward at an angle of 60°, so that the suction surface was upstream of the non-porous section of the attachment-line, as shown in Figure 15. A 4mm diameter two-dimensional trip wire was wrapped around the leading edge of the model 475mm upstream of the suction surface. This ensured that the attachment-line was turbulent and fully developed when it encountered the suction surface. The flow state was monitored using a hot-wire anemometer located at various distances beyond the end of the suction surface. A schematic view of the attachment-line is shown in Figure 16.

For each hot-wire position the suction rate was set and the freestream velocity was increased until the onset of transition.

7.1.1 Transition Onset Criterion

The onset of transition was judged to have occurred when, at constant working section dynamic pressure, two or three turbulent bursts occurred every two seconds.

7.2 Results

The attachment-line state was monitored at four stations: 80mm, 280mm, 490mm and 690mm downstream of the end of the suction surface.

Transition onset data are presented in Figure 17, and it can be seen that, for large values of s, $\overline{R}$ and C_q have an approximately linear relationship until $C_q \approx -0.0032$. For larger suction coefficients, $\overline{R}$ tends to a value that is independent of the suction coefficient. It can be seen that the data from all of the spanwise positions, except those taken at 80mm, approach an asymptotic $\overline{R}$ value of between 740 and 780 (at the 80mm station the relaminarised boundary layer was very stable because the s/η was only approximately 300 at an $\overline{R}$ of 800). The results from the 490mm and 690mm stations show the clearest asymptotic trends, and the maximum s/η values obtained were 1713 and 2300 respectively. The asymptotic $\overline{R}$ value is close to that obtained by Poll [10] for transition onset in the absence of a trip wire. The present experiments were conducted at an s/η of between 150 and 2400, putting them at the lower end of Poll's data, and the results are compared in Figure 18. Extrapolating Poll's data to small s/η, it can be seen that natural transition occurs at values of $\overline{R}$ between 750 and 800, in the s/η range 1713 to 2300,, which are close to the current values. This would suggest that what has been seen is 'natural' transition behaviour (ie the relaminarised attachment-line behaves as though it had never been turbulent). This is different from the situation occurring in two-dimensional flat plate flow, where the relaminarised boundary layer undergoes transition to turbulence almost immediately after the suction is stopped. Due to the three-dimensional nature of the flow at the leading edge of a swept wing, fluid from the

attachment-line boundary layer moves in the chordwise direction is replaced with fluid entrained from the freestream. Therefore, the boundary layer flowing onto the non-porous surface is not composed of the same fluid which was relaminarised on the suction surface.

7.3 Conclusions

A relaminarised attachment-line flowing onto a non-porous undergoes 'natural' transition. Thus, the relaminarised flow behaves like a new laminar boundary layer developing on a smooth surface. This has important implications for the spanwise extent of suction required to maintain laminar flow on a swept wing.

8. A Study of the Effect of Attachment-Line Suction on the Spanwise Propagation of Gross Disturbances in the Wing-Fuselage Junction

Surface suction at the leading edge of swept wings has been used to relaminarise the attachment-line and to control cross-flow transition. One possible application for suction is the suppression of turbulent contamination in the immediate vicinity of the wing-fuselage junction. In this area, the turbulent boundary layer from the fuselage surface wraps around the wing root and a complex flow field develops. A 'horse-shoe' vortex may form in the junction, with one branch on the upper surface of the wing and the other on the lower surface. There may also be a separated region at the root of the wing caused by the large, local pressure gradients. The boundary layer which forms on the leading edge of the wing after the flow has reattached is always turbulent and, this turbulence may propagate in the spanwise direction, contaminating the attachment-line flow. In the past, two devices have been proposed to prevent this contamination. One is the Gaster 'bump', which creates a local stagnation point on the attachment-line, damping the turbulence, and allowing a new laminar boundary layer to form[12]. The other is a suction fence, which stops the spanwise flow and then uses strong suction to prevent flow separation[13]. As with the Gaster bump, a new laminar boundary layer forms the other side of the fence. In the present experiments, leading edge suction was used in the wing-fuselage junction to try to modify the local flow and prevent turbulence propagating along the attachment-line.

8.1 Experimental Method

The model was swept forward at 60°, so that the non-porous section of the attachment-line was downstream of the porous region. For these tests a streamwise endplate was attached to the leading edge to simulate a wing-fuselage junction. This

arrangement is shown in Figure 19. The endplate extended from 0.3m in front of the leading edge to beyond the trailing edge of the model, and spanned the entire working section. A 4mm diameter trip wire was attached to the plate, 10mm downstream of the leading edge, so the boundary layer on the plate approaching the plate/wing junction was fully turbulent. The total suction surface length was 900mm and the state of the attachment-line on the suction surface was monitored at various locations using a hot-wire anemometer. Tests were conducted at fixed freestream speed and the suction rate was increased until relaminarisation had occurred.

8.1.1 Relaminarisation End Criterion

Relaminarisation was judged to have been complete when, at constant working section dynamic pressure, two or three turbulent bursts occurred every two seconds, as in Section 5.

8.2 Results

After several runs, it became clear that, with this configuration, the elimination of all attachment-line turbulence was impossible. At this sweep angle, the $\overline{R}$ could be varied from approximately 400 to 835. Since the boundary layer on the streamwise endplate had been tripped, the attachment-line was turbulent at all values of $\overline{R}$ for the experimental arrangement. Using the entire suction surface (900mm) complete relaminarisation could not be achieved at the highest suction levels available (C_q=-0.0339). Figure 20, parts (a) to (e), show sampled signals, from the hot-wire, for increasing suction, at $\overline{R} \approx 518$ and $s/\eta \approx 2490$. From work on relaminarising turbulent attachment-line flows (see Section 5) this value of s/η exceeds the value required for asymptotic suction. Figure 20(e) shows that even at a suction coefficient of -0.0339 (which is over ten times the suction coefficient required to relaminarise a fully turbulent, infinite swept, attachment-line at this $\overline{R}$) the intermittency had only been reduced to 0.3. However, the suction coefficient required to eliminate all attachment-line turbulence, at $\overline{R} \approx 518$ and $s/\eta \approx 2490$, can be estimated from this data. The variation of intermittency with suction coefficient is plotted in Figure 21. Fitting a trend to this data shows that a fully laminar attachment-line ($\Gamma=0$) could be obtained with a suction coefficient of approximately -0.07.

8.2.1 The Flow Field in the Wing-Fuselage Junction Region

The flow field in the junction region has been studied by Bergin[14]. He investigated the variation of $\overline{R}$ along the leading edge in the region of the wing-fuselage junction and his results are given in Figure 22. It can be seen that for a sweep

angle of 60°, $\overline{R}$ reaches the infinite swept value at s/D≈1.6. The effect of the suction on the infinite swept attachment-line is, therefore, modified. In the current tests the non-infinite swept region was 650mm, so only 250mm of the suction surface was acting on an infinite swept attachment-line.

With this information the results become clear. With the arrangement used, surface suction was incapable of completely eliminating all turbulence in the junction, up to approximately s/D≈1.6. Because the experimental $\overline{R}$ was larger than 250 (the approximate value obtained by Poll for the propagation of turbulence along a swept attachment-line) some turbulence had to be removed by the remaining length of suction surface, which was only 250mm long. This corresponds to $s/\eta \approx 692$. From the empirical relations given by Danks and Poll (see Section 5.3.1), at $s/\eta=692$ and $\overline{R}=518$ the suction coefficient required would be $C_q \approx -0.0085$. This is smaller than the largest suction coefficient used but this is probably due to a number of factors.

As noted by Bergin, the non-dimensional distance from the junction that infinite-swept conditions stabilise depends on the sweep angle and the state of the end-plate boundary layer, particularly its thickness. The plate boundary layer was laminar during Bergin's experiments but was turbulent for the current tests and, for the arrangement used in the current tests, a turbulent boundary layer on the flat plate would be four times thicker than an equivalent laminar layer. According to Barber[15] the larger the boundary layer thickness the larger the region of influence of the wing-fuselage vortex, although no quantitative measure of the effect is given. Therefore, the effective s/η was probably smaller than that calculated above and the suction coefficient predicted from Danks and Poll would be larger.

Also, the $\overline{R}$ used here was greater than that used in Bergin's experiments (518 compared with 360), so the vortex was probably stronger and the region of influence larger again, leading to a smaller effective s/η.

8.3 Conclusions

For the experimental arrangement used, the attachment-line could not be fully relaminarised using suction in the immediate vicinity of the wing-fuselage junction, even using very large suction coefficients.

Previous work, also at a sweep angle of 60°, has shown that flow conditions are not effectively infinite swept until at least 1.6 diameters downstream of the plate/cylinder junction and this reduces the effectiveness of suction in the junction area.

9. The Effect of Blowing on the Attachment-Line Boundary Layer

The object of these surface transpiration experiments is to provide data which can be used to design systems that can be incorporated into aircraft. Surface suction is a very efficient method of boundary layer control but attention must be paid to the

consequences of a failure of the system. Such a failure might result in a reversal of the flow direction, ie blowing rather than suction. Therefore, some tests were performed to establish the effect of blowing on the state of the attachment-line boundary layer.

9.1 Experimental Method

The model was set at a sweep angle of 55°, as in Figure 5. The state of the attachment-line was monitored 739mm downstream of the start of the porous surface by a hot-wire anemometer. Blowing was applied using a small compressor.

9.1.1 Transition Criterion

The onset of transition can be characterised in the same way as the end of relaminarisation. The same criterion was used for these experiments as for the relaminarisation tests: ie the onset of transition was considered to have occurred when, at constant working section dynamic pressure, two or three turbulent bursts occurred every two seconds.

9.2 Results

The blowing results are given in Figure 23. It can be seen that as the transpiration coefficient increases, the value of $\overline{R}$ required for transition onset decreases, as would be expected. Interpolating the results to the zero blowing case gives a $\overline{R}$ of approximately 650 at $s/\eta \approx 10000$. Referring to Poll's work on transition in the absence of a trip wire[10], at large s/η the $\overline{R}$ required for the onset of natural transition is between 600 and 650, which agrees well with the present result. Previous work by Poll, Danks and Yardley[16] is compared with the current work in Figure 24. There is excellent agreement between the two sets of data. It is interesting to note that, as the blowing coefficient increases, the rate of change of $\overline{R}$ decreases, suggesting that there may be an asymptotic value of $\overline{R}$, below which blowing will never cause transition. Further tests are required to check this. However, the model used in these tests cannot be used at these extreme conditions.

9.2.1 Comparison With Stability Analysis

A linear stability analysis on the effect of blowing at the attachment-line boundary layer has been performed by Theofilis[17]. Calculations were made for a range of blowing coefficients and from these the stability envelope of the boundary layer can

be found. For a given blowing coefficient, the boundary layer can be in one of three states:

1) Stable, where the amplitude of a small disturbance decreases with increasing spanwise location (ie the boundary layer will remain laminar)
2) Unstable, where the amplitude of the disturbance increases with increasing spanwise location and transition will eventually occur
3) Neutrally stable, where the amplitude of the disturbance neither increases nor decreases. It should be noted that when the flow is neutrally stable no disturbance is visible if the flow is monitored (eg with a hot-wire).

The linear stability envelope for $\overline{R}$ =350 is given in Figure 25. The spatial amplification rate, α_i , is a measure of the stability of the boundary layer. For $\alpha_i > 0$, the flow is stable, for $\alpha_i < 0$ the flow is unstable, and $\alpha_i = 0$ is the special case of neutral stability. The frequency used in stability analysis is a non-dimensional term, and is related to the actual frequency by

$$F = \left(10^6 .2\pi . \frac{\nu}{V_e^2} \right) f$$

The frequency of the most amplified disturbance can, therefore, be found from Figure 25, as that for which α_i is a minimum for each blowing coefficient. Also, as the blowing coefficient increases, the range of frequencies that are amplified increases. As the blowing coefficient increases and the magnitude of the amplification rate increases, disturbances at frequencies associated with harmonics of the fundamental most amplified frequency may appear as well [16]. In Figure 25, it can be seen that, as the blowing coefficient increases, the frequency of the most amplified disturbance changes only slightly, and this is the case for blowing on an infinite swept attachment-line.

In the experiment the most amplified disturbance is clearly visible and an example is shown in Figure 26. To assess the correspondence between linear stability theory and experiment the output signal of the hot-wire was digitally sampled when a laminar disturbance was visible The experimental conditions were: $\overline{R}$ =372, C_q=0.000349, and $s/\eta \approx 1900$ (where s is the distance between the hot-wire and the start of the porous surface). The signal was then manipulated using a Fast Fourier Transform (FFT) algorithm to obtain the amplitude spectrum. This spectrum, low passed to a frequency of 5kHz, is shown in Figure 27. It can be seen that the peak disturbance frequency occurs at approximately 750Hz, with a second, smaller, peak at approximately 1500Hz (ie twice the frequency of the main peak) and a third, smaller, peak at 380Hz (half the frequency of the main peak). From Theofilis' analysis, the frequency of the most amplified disturbance under these conditions would be approximately 730Hz, which is very close to the frequency of the observed disturbance.

9.3 Conclusions

Small blowing coefficients have a large destabilising effect on the laminar attachment-line boundary layer.

The results suggest that there may be an asymptotic $\overline{R}$ limit below which blowing will not cause transition, but further tests would be required to prove this.

Excellent agreement with previous experimental work has been achieved, and the results agree with predictions from linear stability theory.

Conclusions

The conditions required to relaminarise a fully turbulent attachment-line have been investigated up to $\overline{R}$ values of 1000. It was found that, in the limit of $s/\eta \rightarrow \infty$, at constant $\overline{R}$ the suction coefficient required for relaminarisation tends to an asymptotic value. Also, it was found that there exists a suction coefficient at which turbulent attachment-line flow is impossible, at all values of $\overline{R}$ and this is $C_q \approx -0.0033$.

Critical oversuction, an effect caused by very large suction levels introducing large disturbances into the boundary layer and causing transition to occur at a lower $\overline{R}$ than without suction, has been investigated. It was found that even with a C_q of -0.100 no adverse effects were seen. Data from a previous investigation were re-examined and compared with an empirical criterion taken from two-dimensional work by Ellis. It was found that the data did not exceed Ellis's criterion, whereas data from the current work did.

The retransition which occurs when a relaminarised attachment-line flows onto a non-porous surface was studied. It was found that, at large s/η, the $\overline{R}$ for retransition onset approached an asymptotic value independent of the suction coefficient used for relaminarisation. Transition onset occurred at $\overline{R} \approx 760$ which, at $s/\eta \approx 2400$, agrees very well with work by Poll, for transition in the absence of a trip wire. Therefore, it seems that a relaminarised attachment-line flowing onto a non-porous surface behaves as though it had never been turbulent and undergoes 'natural' transition behaviour.

Suction was applied in the immediate vicinity of a wing-fuselage junction. It was found that, for the experimental arrangement used, the attachment-line could not be fully relaminarised, even using suction levels ten times larger than those required for infinite swept conditions.

Finally, attachment-line blowing has been investigated. The results agree well with previous work. The laminar attachment-line is very sensitive to blowing and this highlights the danger of a fault occurring in the suction system during flight, causing a reversal in the transpired flow. The results indicate that, at small $\overline{R}$, an asymptotic $\overline{R}$ limit exists below which blowing can not cause transition. This limit is probably at an $\overline{R}$ between 150 and 200.

References

[1] Gray, W E: ***The effect of wing sweep on laminar flow***. RAE Technical Memo 255, 1952

[2] Owen, P R and Randall, D G: ***Boundary layer transition on a swept back wing***. RAE Technical Memo 277, 1952

[3] Nitsche, W and Szodruch, J: ***Concepts and results for laminar flow research in wind tunnel and flight experiments***. ICAS Conference Proceedings, 1990

[4] Danks, M and Poll, D I A: ***Final report for contract NAGW-3871 transition of flow at and near an attachment-line - including control by surface suction***. Aerospace Division, Manchester School of Mechanical Engineering, University of Manchester, April 1995

[5] Poll, D I A: **Transition in the infinite swept attachment-line boundary layer**. *The Aeronautical Quarterly*, Vol. XXX, November 1979

[6] Gregory, N and Stuart, J T and Walker, W S: ***On the stability of three-dimensional boundary layers with application to the flow due to a rotating disc***. Philosophical Transactions of the Royal Society of London, Series A, Vol. 248, pp155-199

[7] Emmons, H W: **The laminar-turbulent transition in a boundary layer, part 1**. *Journal of Aerospace Sciences*, Vol. 18, 1951, pp490-498

[8] Pfenninger, W: ***Flow problems of swept low drag suction wings of practical construction at high Reynolds numbers***. Lecture Presented at Subsonic Aeronautics Meeting, New York, April 1967

[9] Gaster, M: **On the flow along swept leading edges**. *Aeronautical Quarterly*, May 1967

[10] Poll, D IA: ***Some aspects of the flow near a swept attachment-line with particular reference to boundary layer transition***. PhD Thesis, Cranfield Institute of Technology, UK, 1978

[11] Ellis, J: ***Laminar and laminarising boundary layers by suction through perforated plates***. 2nd European Forum on Laminar Flow Technology, Bordeaux, June 1996

[12] Gaster, M: **A simple device for preventing contamination on swept leading edges**. *Journal of the Royal Aeronautical Society,* Volume 69, p788, November 1965

[13] Pfenninger, W: ***Laminar flow control - laminarization.*** Special Course on Concepts for Drag Reduction, AGARD Report 654, March 1977

[14] Bergin, A: ***Transition characteristics of a swept cylinder in the presence of a large streamwise end-plate.*** ICAS-90-7.9.1, ICAS Conference Proceedings, 1990

[15] Barber, T J: **An investigation of strut-wall intersection losses.** *Journal of Aircraft*, Vol. 15, No. 10, 1968, pp676-681

[16] Poll, D I A and Danks, M and Yardley, M R: ***The effects of suction and blowing on stability and transition at a swept attachment-line.*** Proceedings of the Colloquium 'Transitional Boundary Layers in Aeronautics', Royal Netherlands Academy of Arts and Science, 1996

[17] Theofilis, V: Private communication

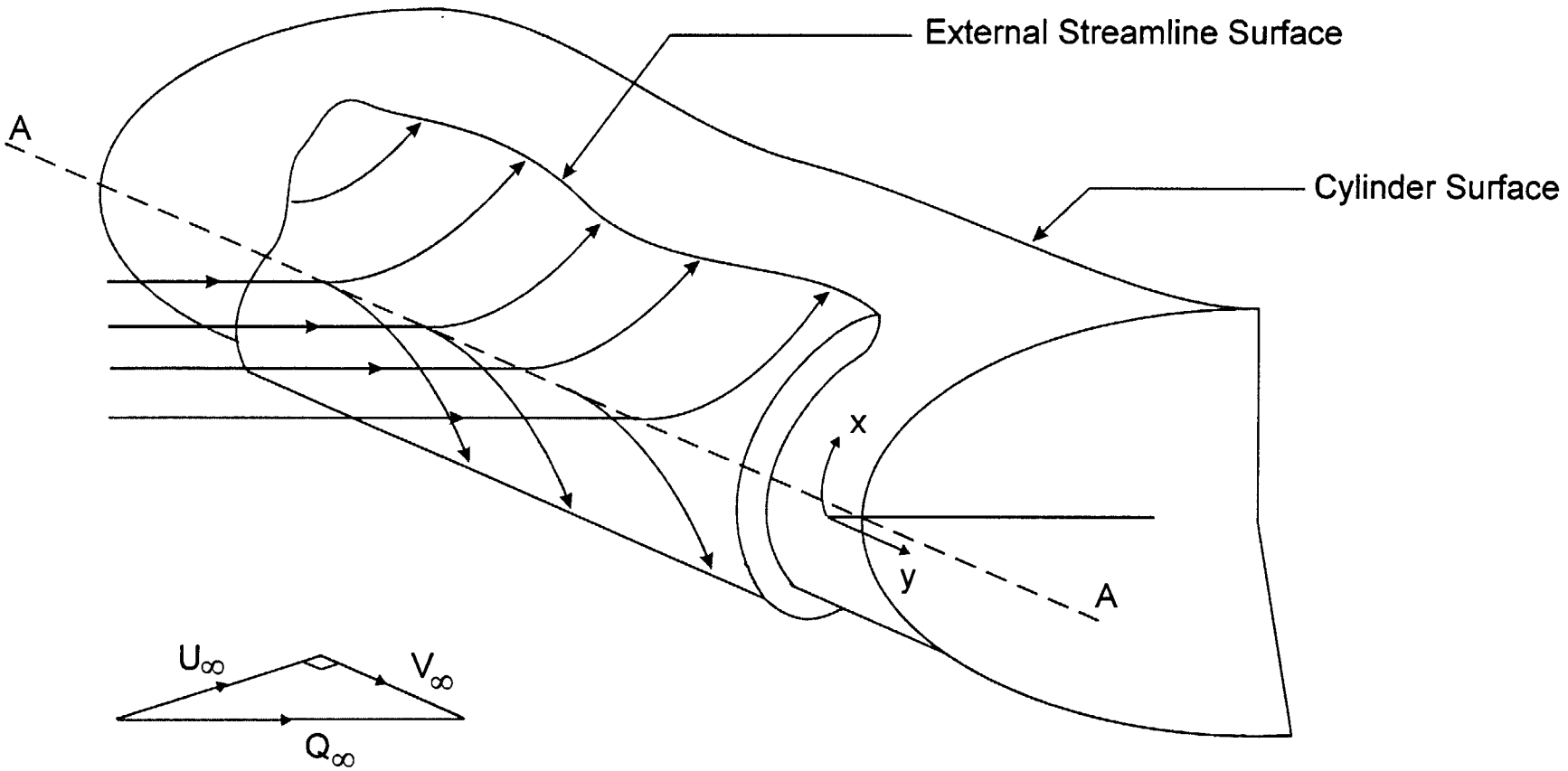

Figure 1. The Flow Near The Leading Edge of a Swept Wing

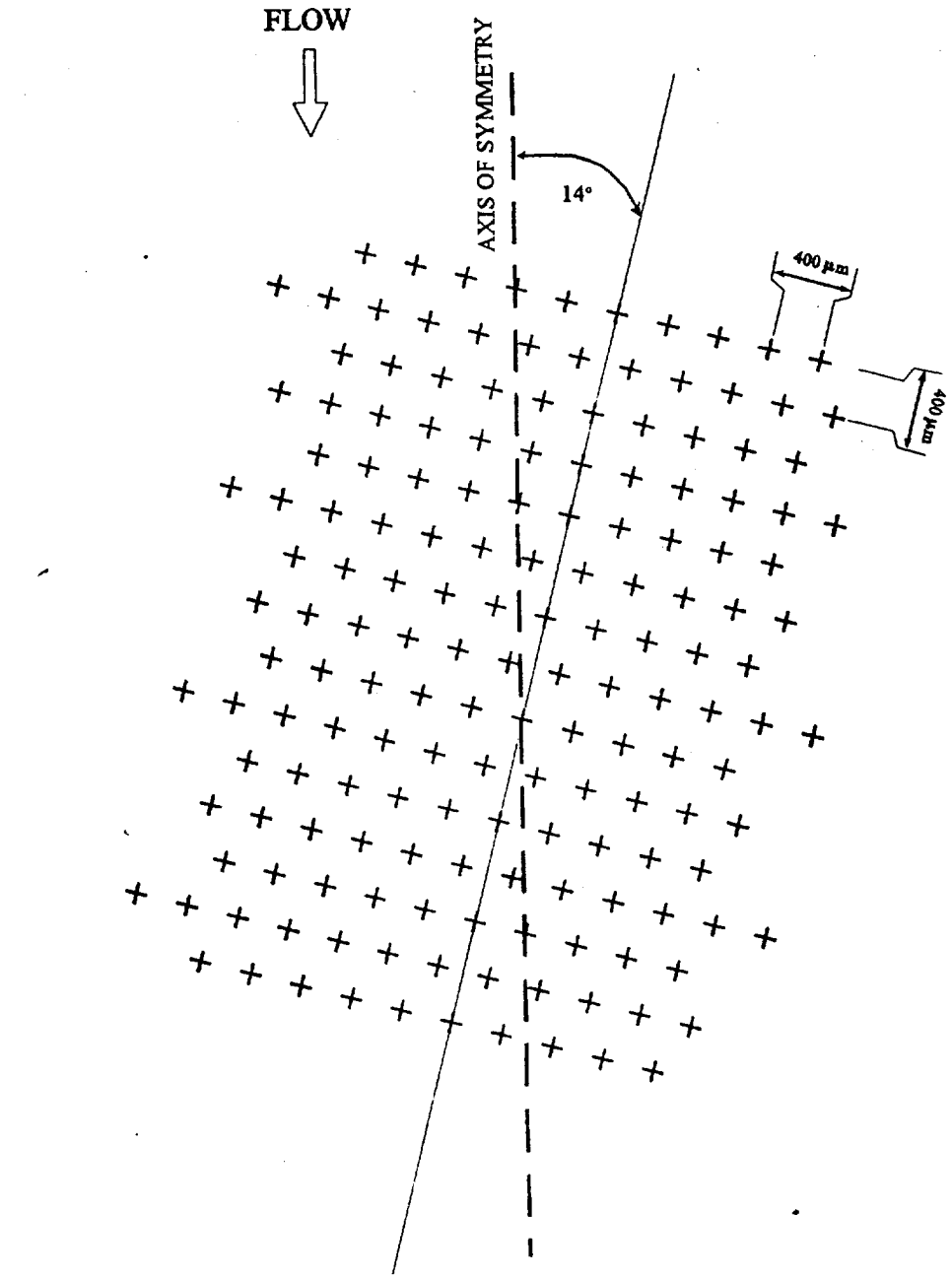

Figure 2. Leading Edge Perforation Pattern

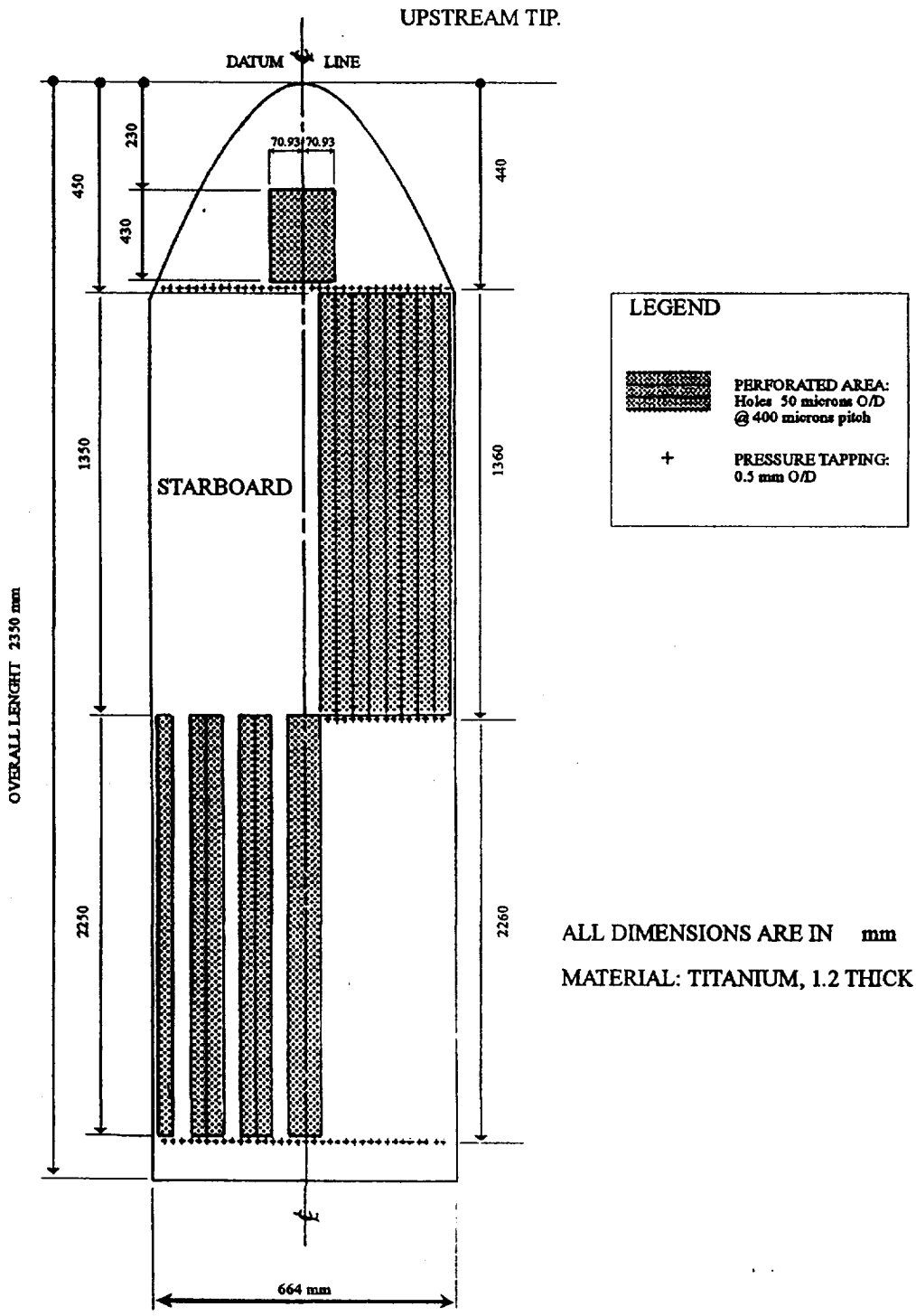

Figure 3. Distribution of Perforated Areas on Titanium Leading Edge

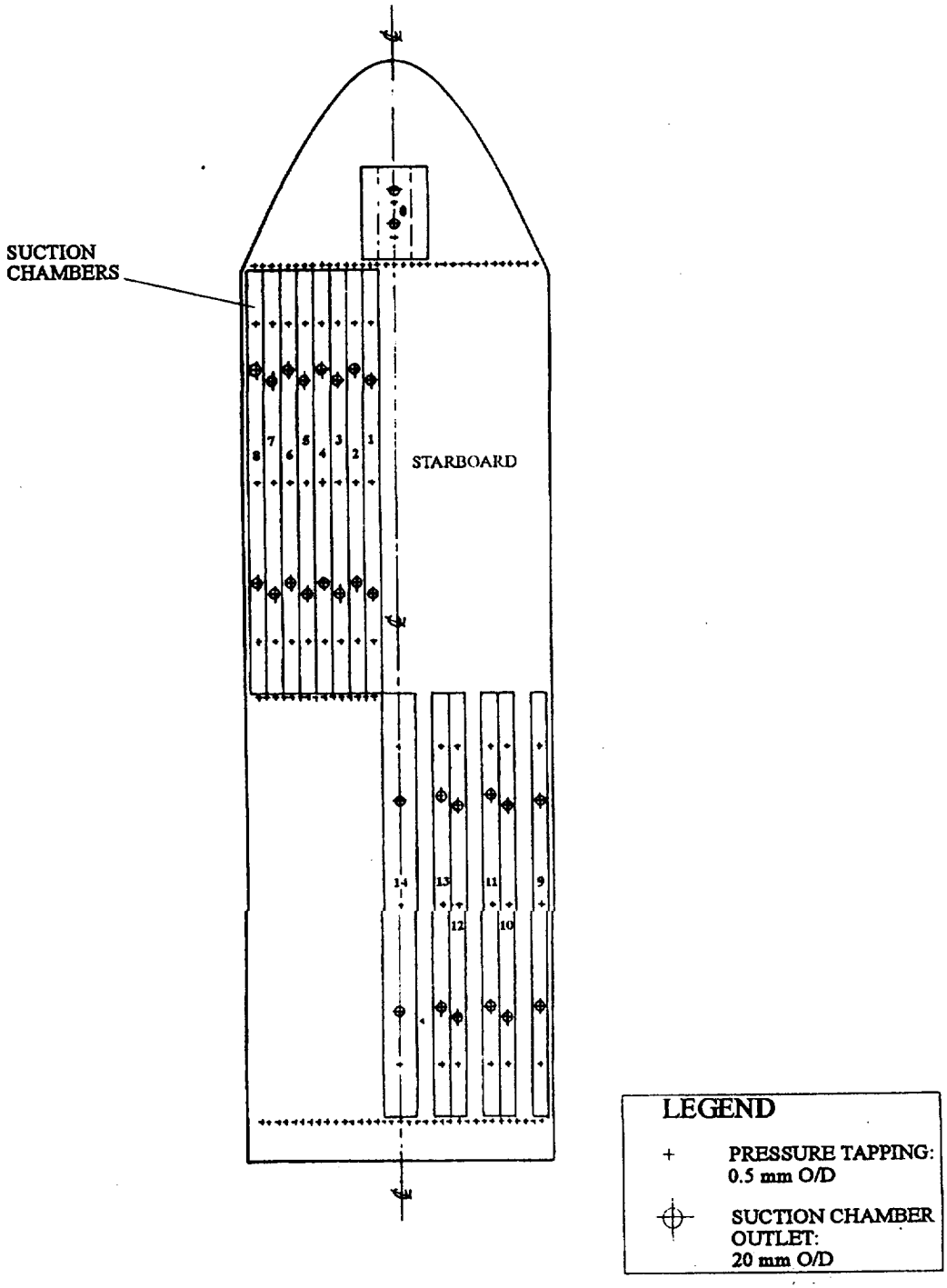

Figure 4. Distribution of Suction Chambers Within the Perforated Titanium Leading Edge Surface

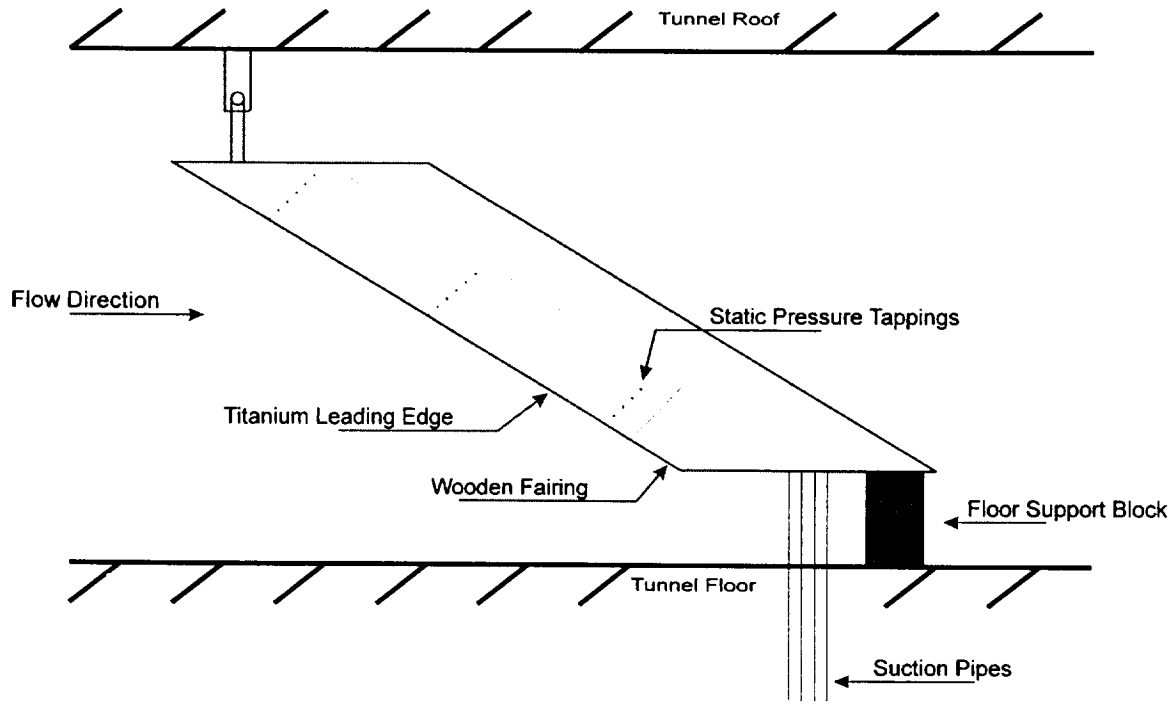

Figure 5. Arrangement of Model in 8'x6' Wind Tunnel

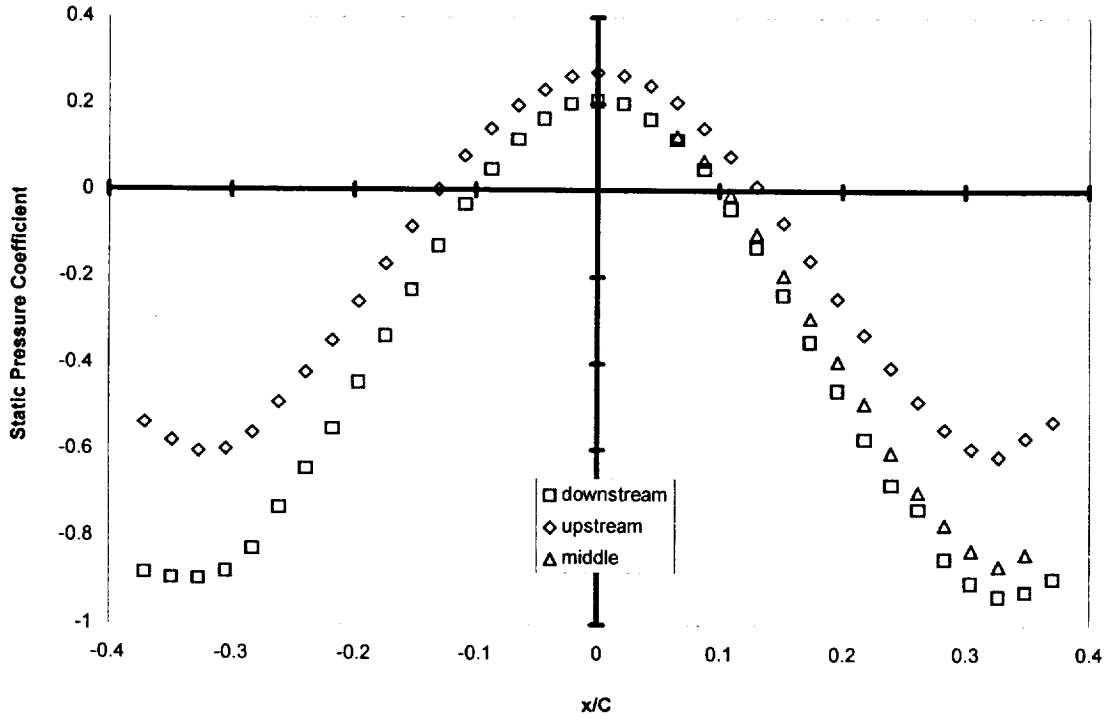

Figure 6. Example Static Pressure Coefficient Distribution Around Cylinder Leading Edge

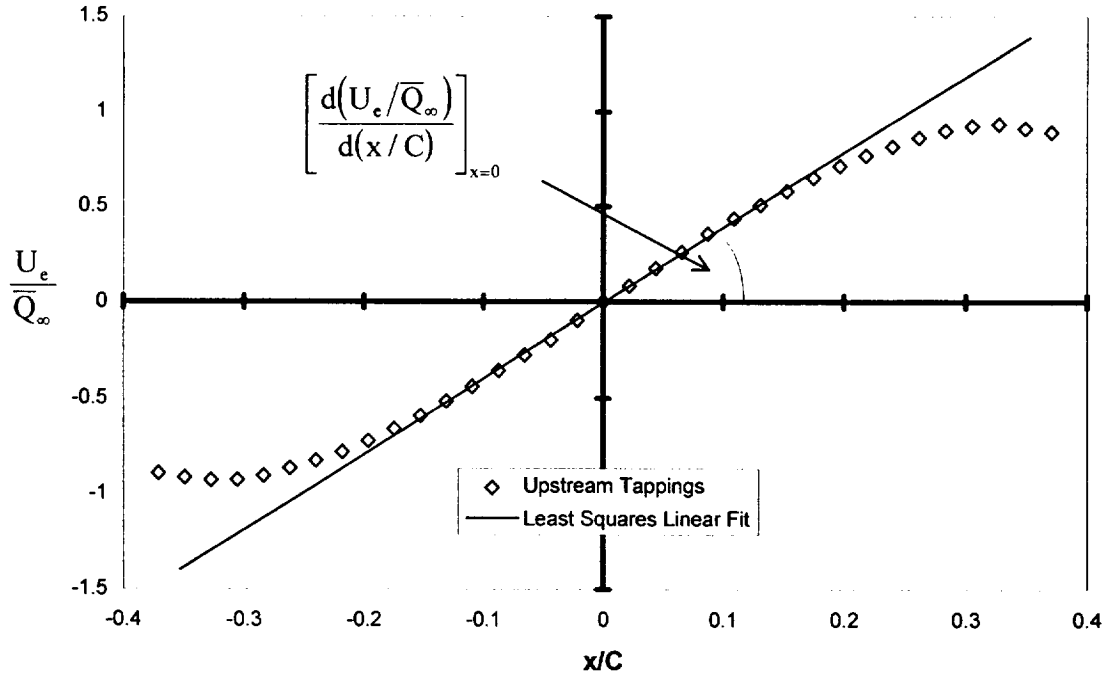

Figure 7. Typical Chordwise Velocity distribution

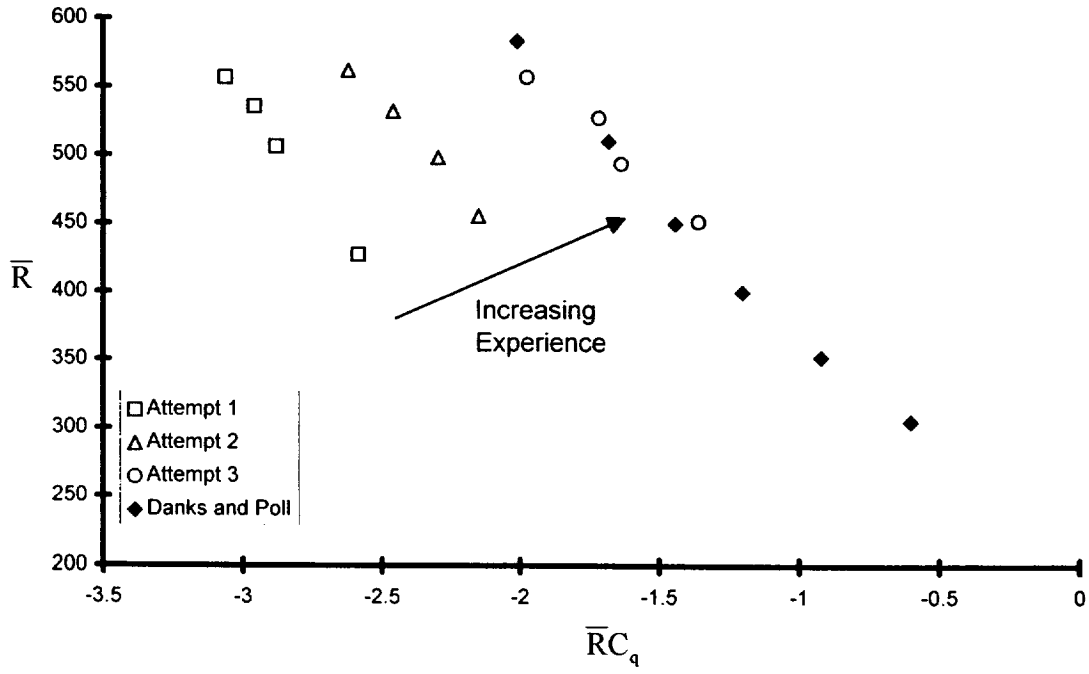

Figure 8. Example of the Effect of Operator Experience on the Data for Relaminarisation

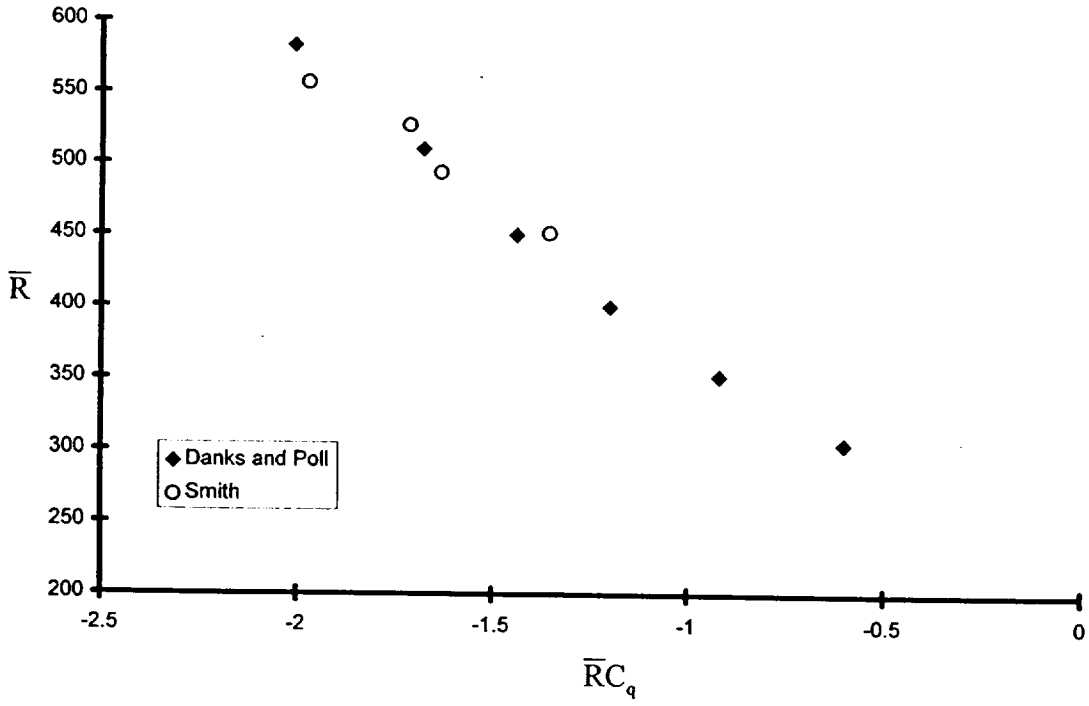

Figure 9. Comparison Between Present Work (Cranfield 8'x6' Tunnel) and Previous Results (Manchester 9'x7' Tunnel)

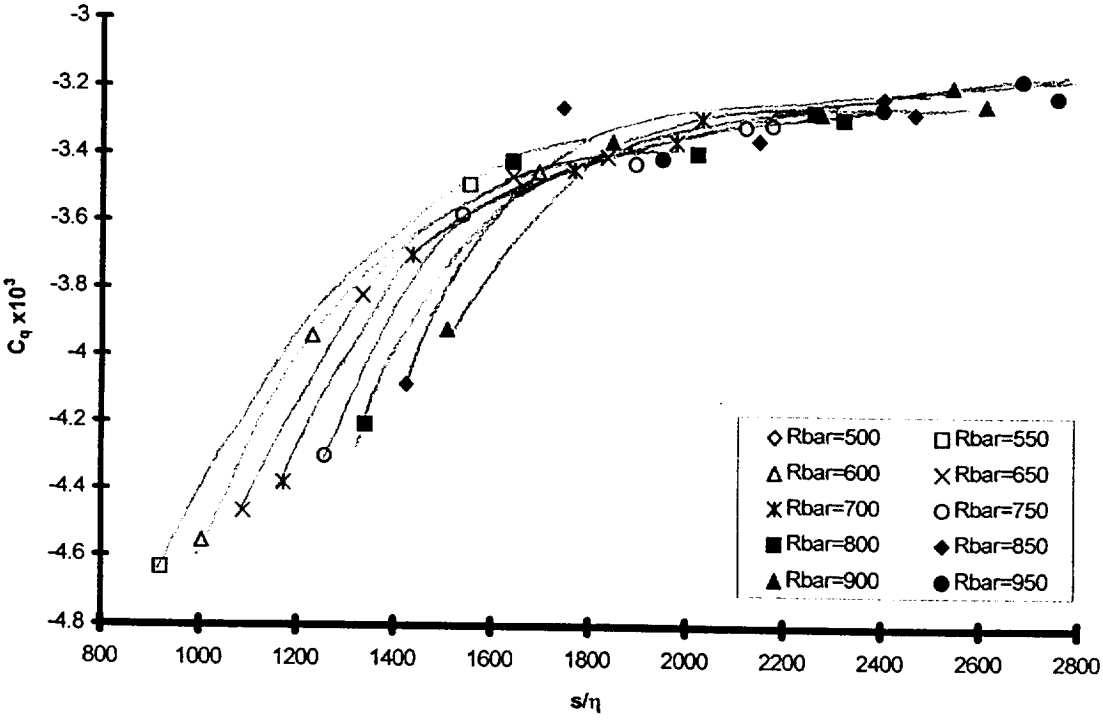

Figure 10. Critical Suction Rate For the End of Relaminarisation (at Constant $\overline{R}$)

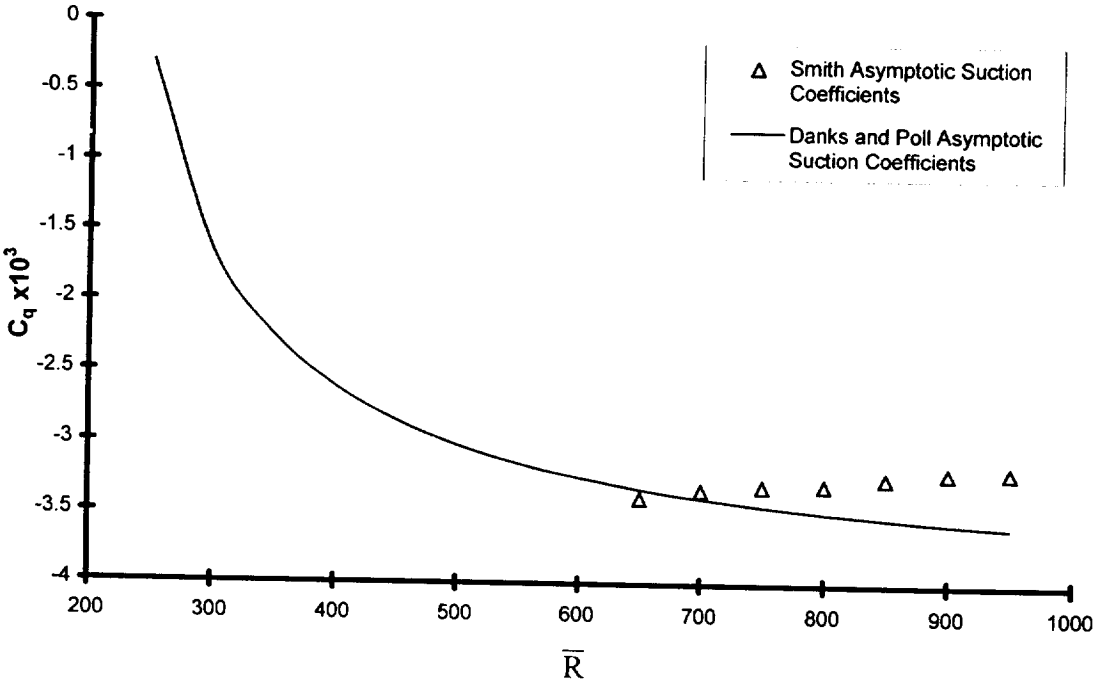

Figure 11. Comparison Of Asymptotic Suction Coefficient Results With Danks and Poll

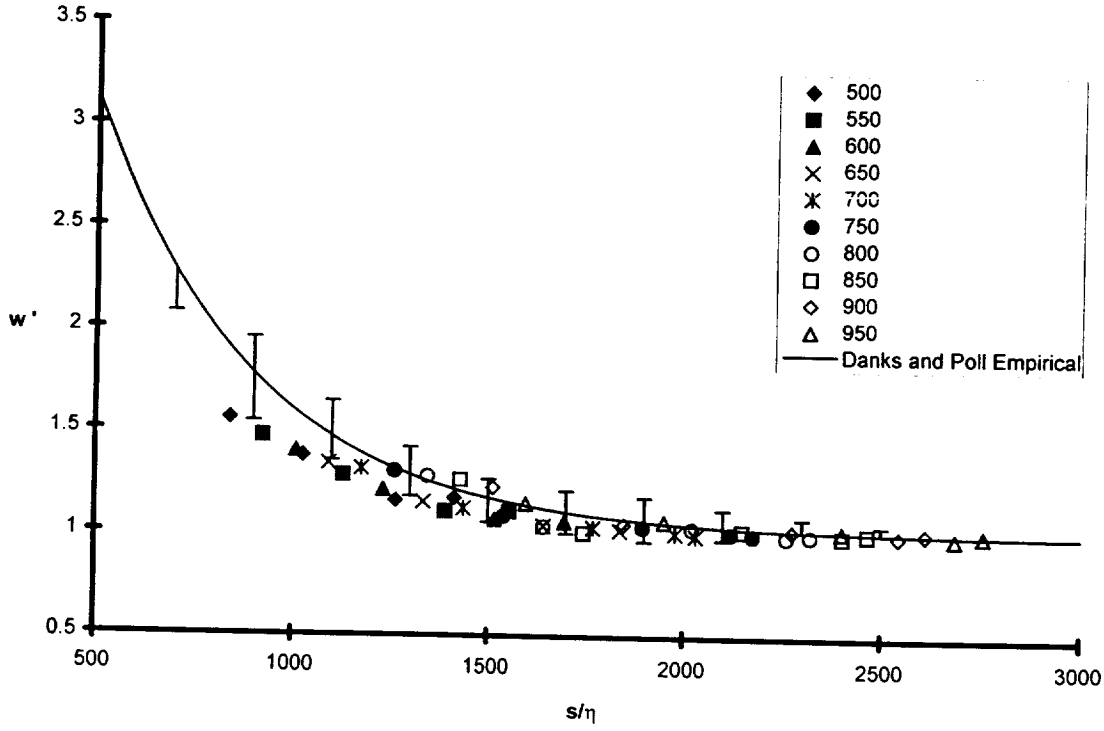

Figure 12. Normalised Suction Rate as a Function of Streamwise Distance (at Constant $\overline{R}$)

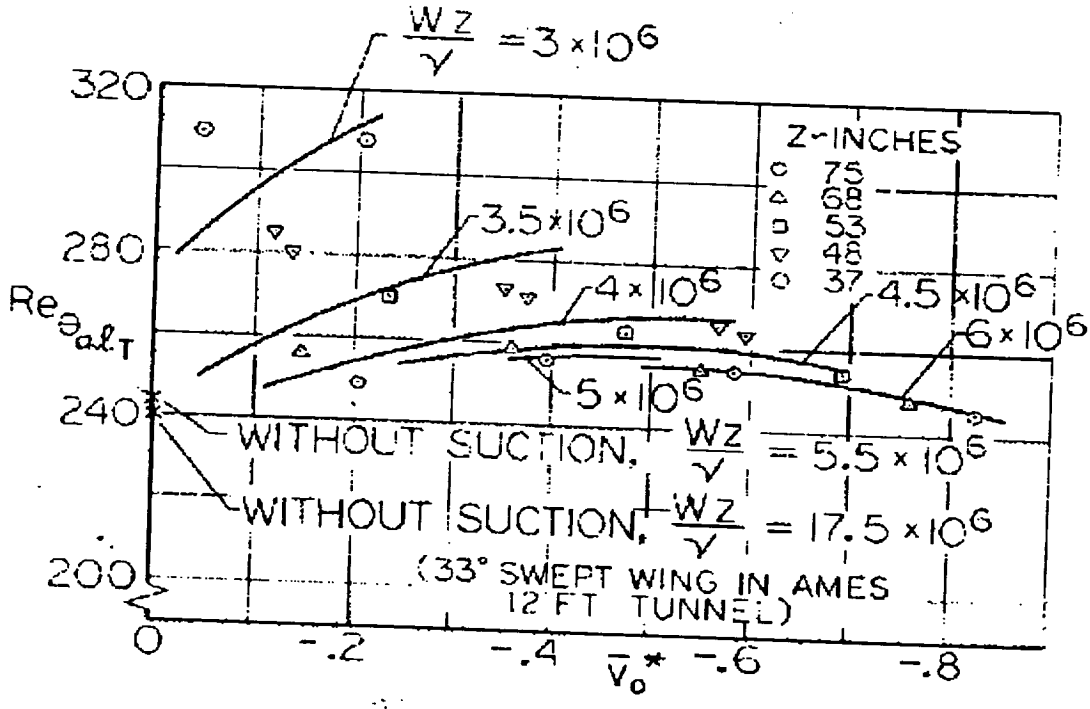

Figure 13. The Beginning of Transition on the 45° Swept Blunt-Nosed Wing For Different Spanwise Length Reynolds Numbers, From Pfenninger

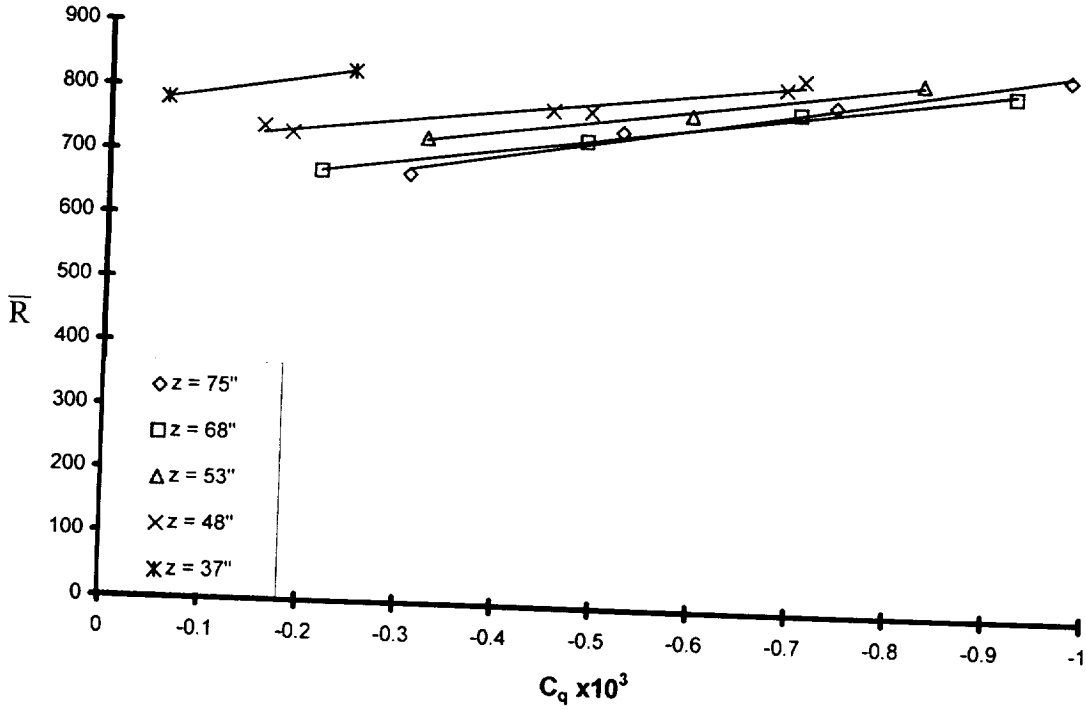

Figure 14. The Beginning of Transition at the Leading Edge of a 45° Swept Blunt-Nosed Wing for Different Spanwise Lengths, From Pfenninger

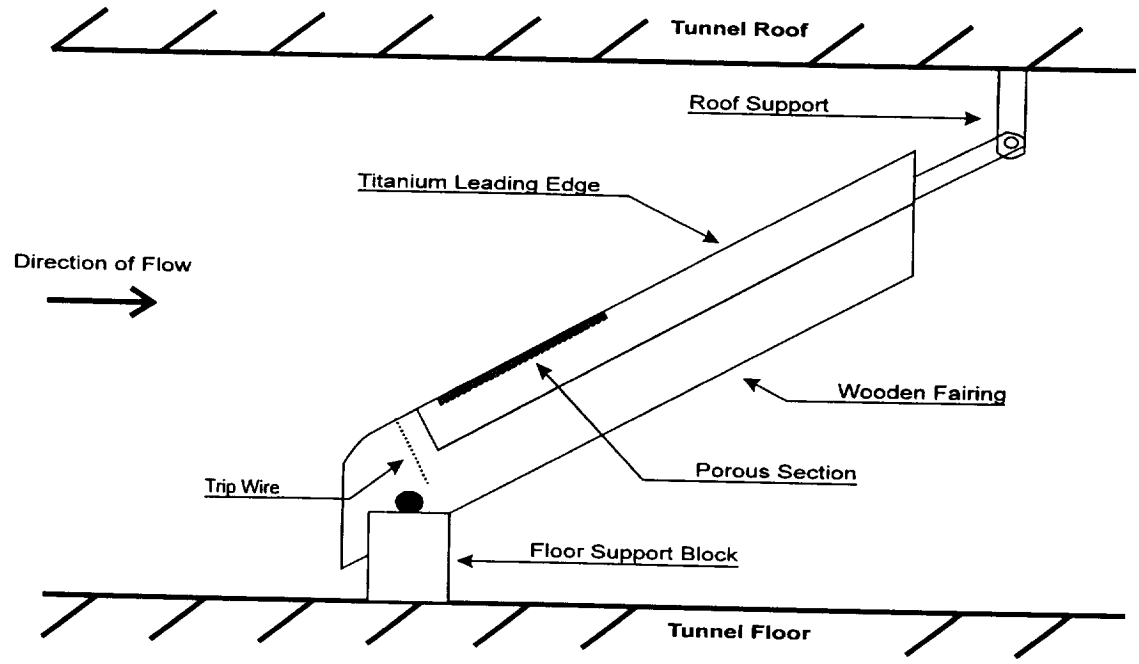

Figure 15. Arrangement of Model Swept Forward in the Wind Tunnel

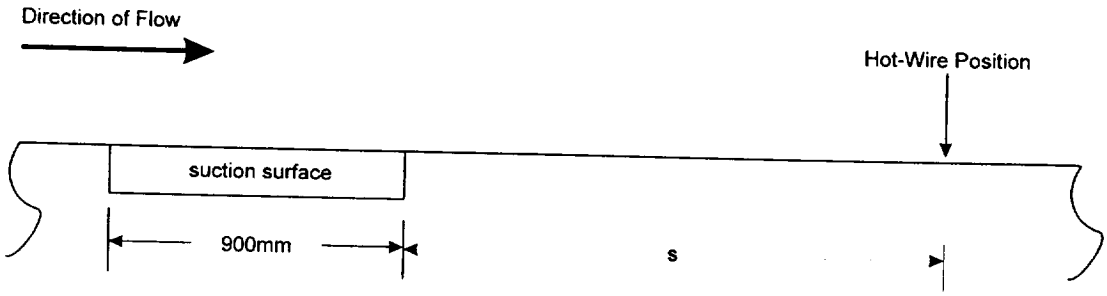

Figure 16. Schematic of Attachment-Line Arrangement During Non-Porous Surface Experiments

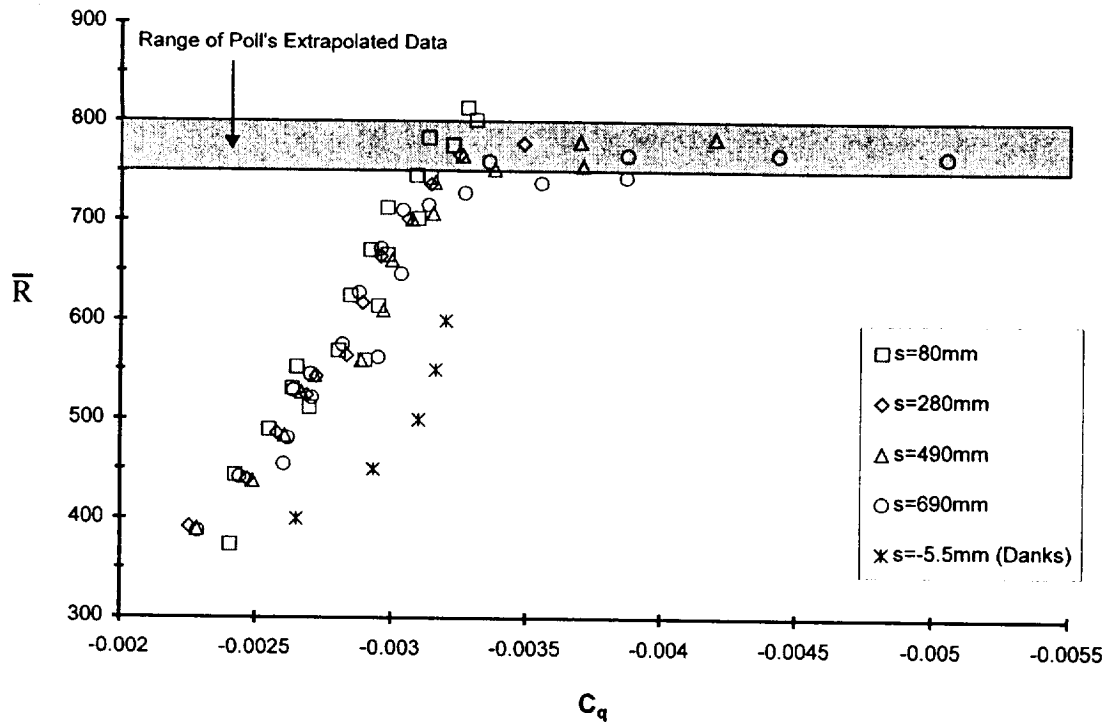

Figure 17. Transition Characteristics of a Relaminarised Attachment-Line Flowing Onto a Non-Porous Surface

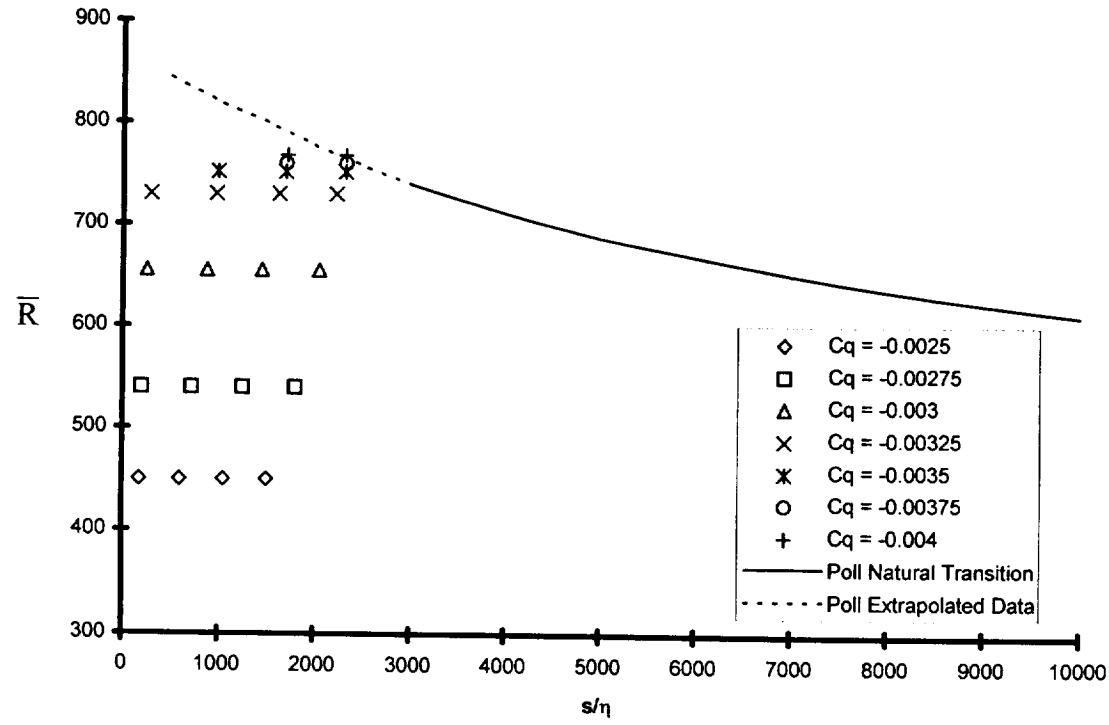

Figure 18. The Effect of Spanwise Distance on the Transition Characteristics of a Relaminarised Attachment-Line Which Flows Onto a Non-Porous Surface

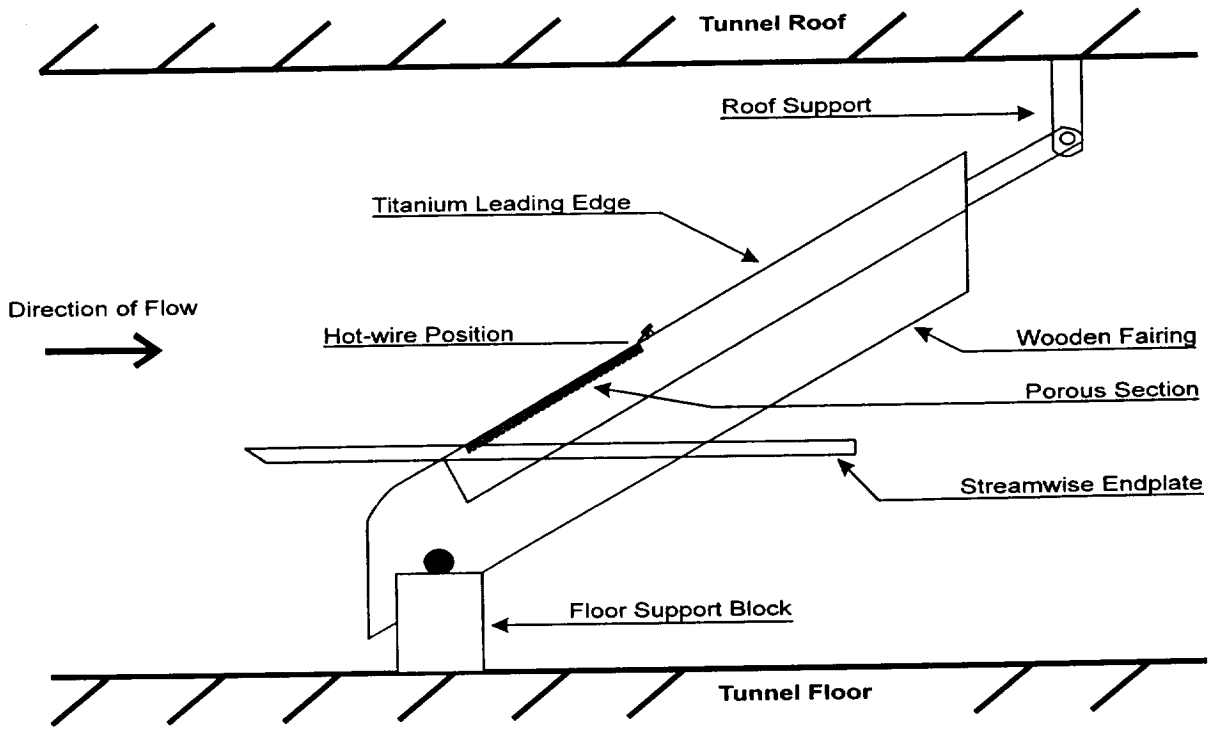

Figure 19. Arrangement of the Model in the Wind Tunnel During the Wing-Fuselage Junction Experiments

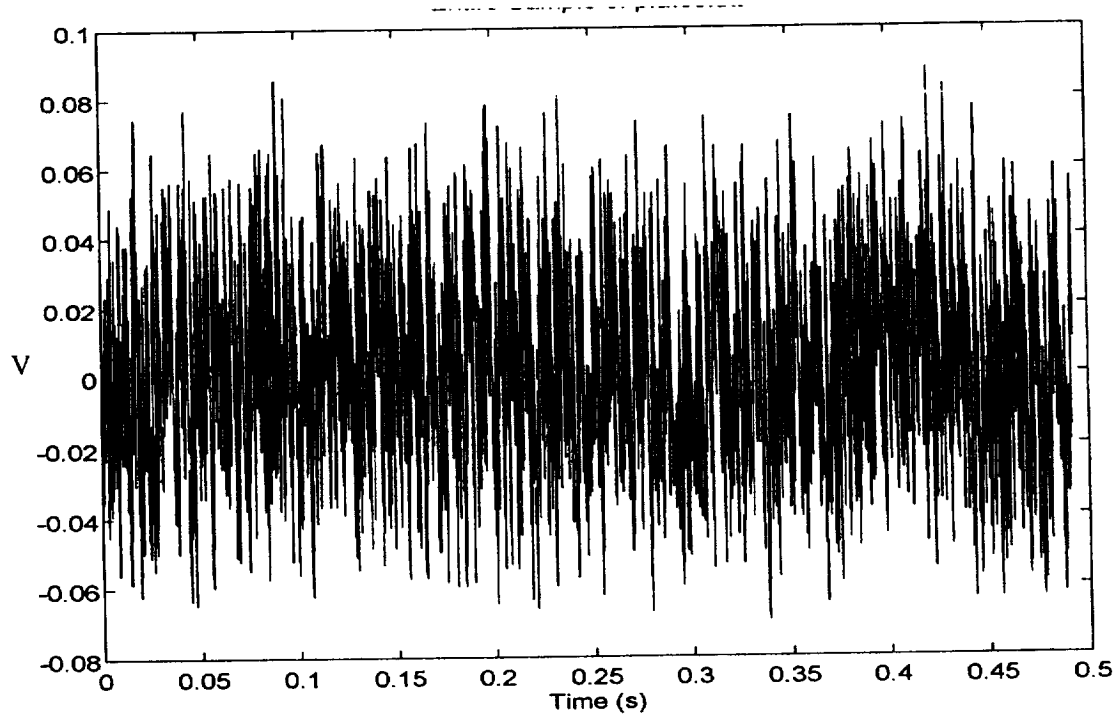

Figure 20(a). Hot-Wire Signal of Attachment-Line Downstream of Wing-Fuselage Junction - $\overline{R}$ =518, s/η=2490, s/D=2.2, C_q=0

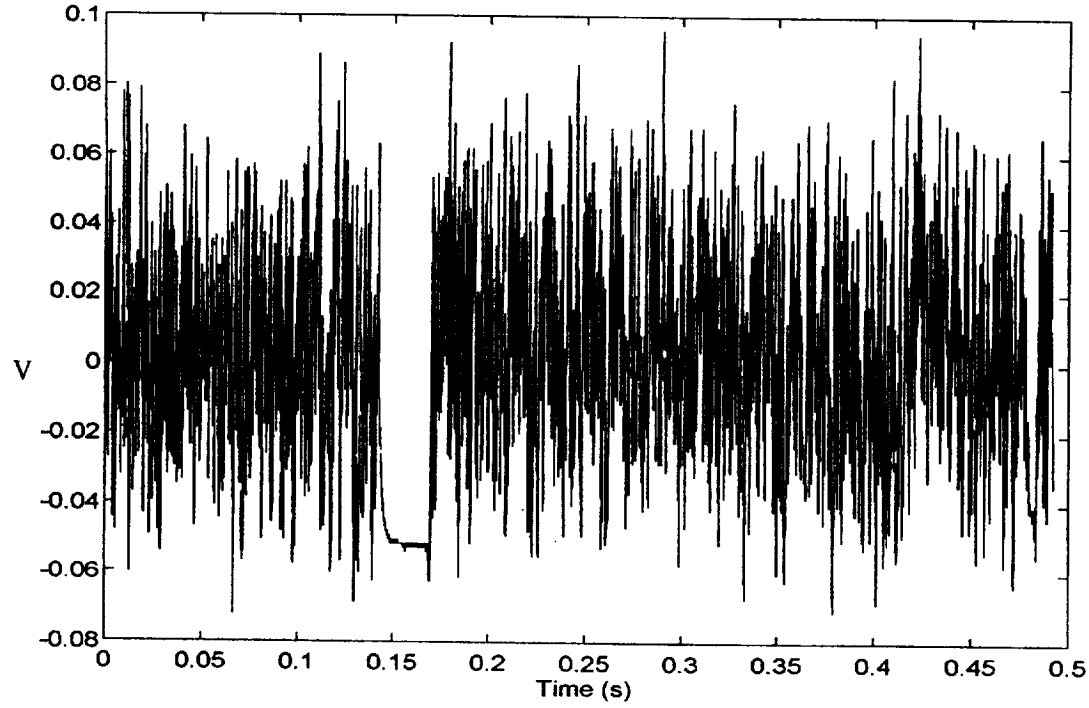

Figure 20(b). Hot-Wire Signal of Attachment-Line Downstream of Wing-Fuselage Junction - $\overline{R}$ =518, s/η=2490, s/D=2.2, C_q=0.00465

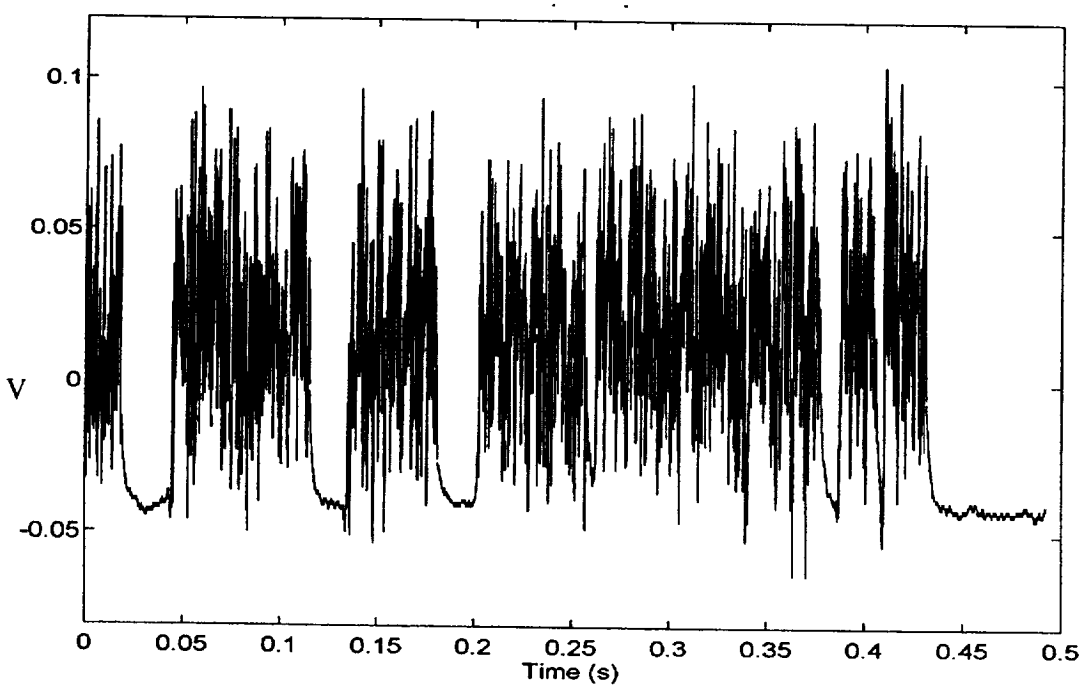

Figure 20(c). Hot-Wire Signal of Attachment-Line Downstream of Wing-Fuselage Junction - $\overline{R}$ =518, s/η=2490, s/D=2.2, C_q=0.00623

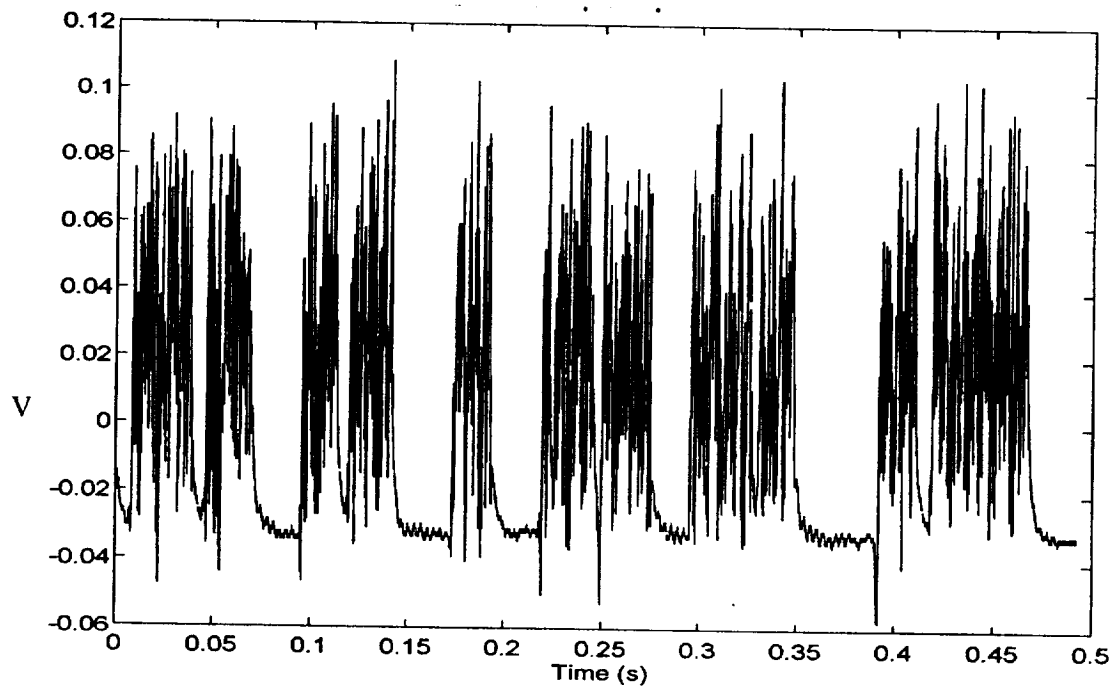

Figure 20 (d). Hot-Wire Signal of Attachment-Line Downstream of Wing-Fuselage Junction - $\overline{R}$ =518, s/η=2490, s/D=2.2, C_q=0.0151

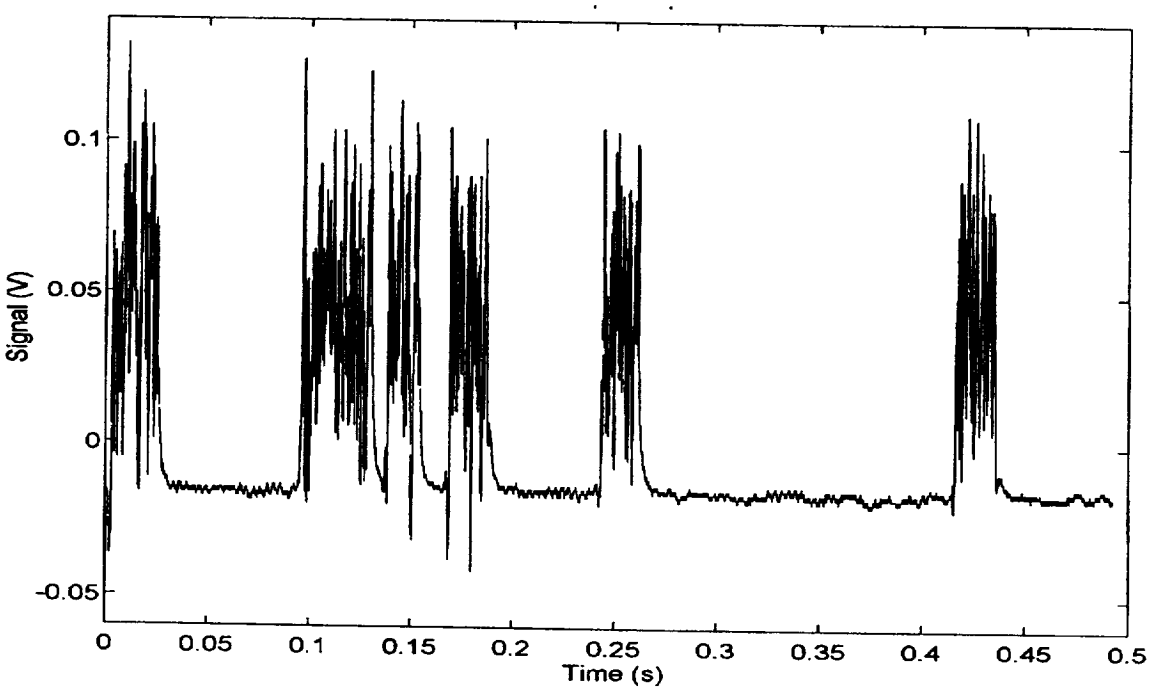

Figure 20 (e). Sampled Hot-Wire Signal of Attachment-Line Downstream of Wing-Fuselage Junction - $\overline{R}$ =518, s/η=2490, s/D=2.2, C_q=0.0339

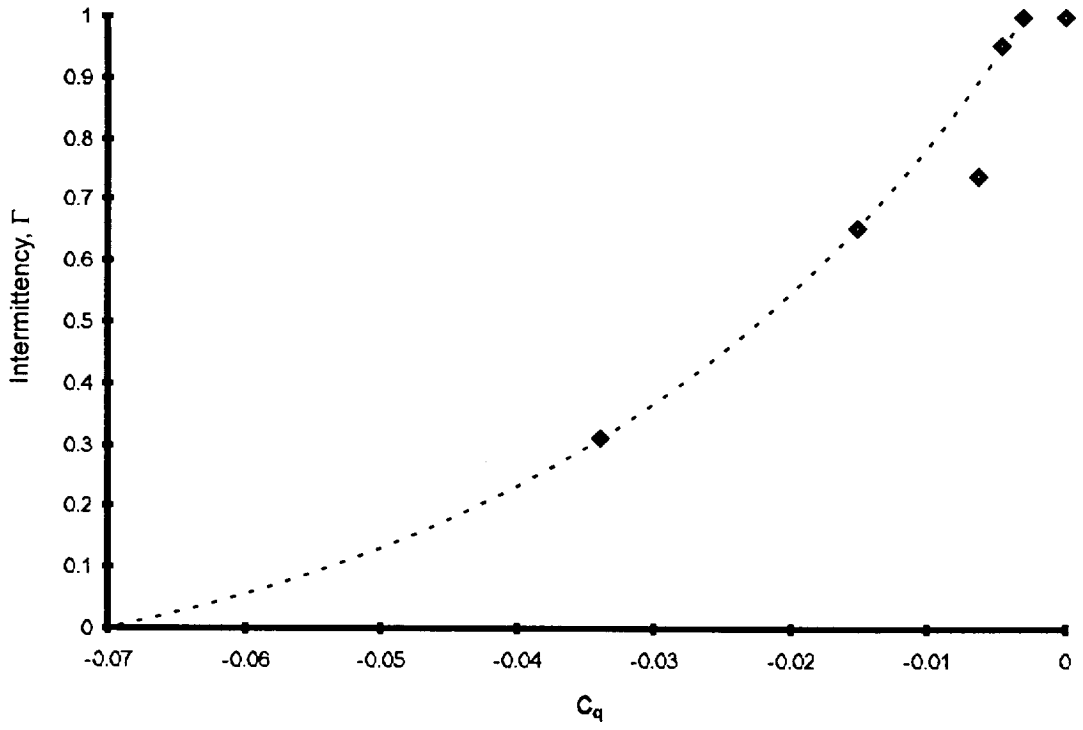

Figure 21. The Variation of Intermittency With Suction Coefficient in the Wing-Fuselage Junction; $\overline{R}$ =518, s/η=2490, s/D=2.2

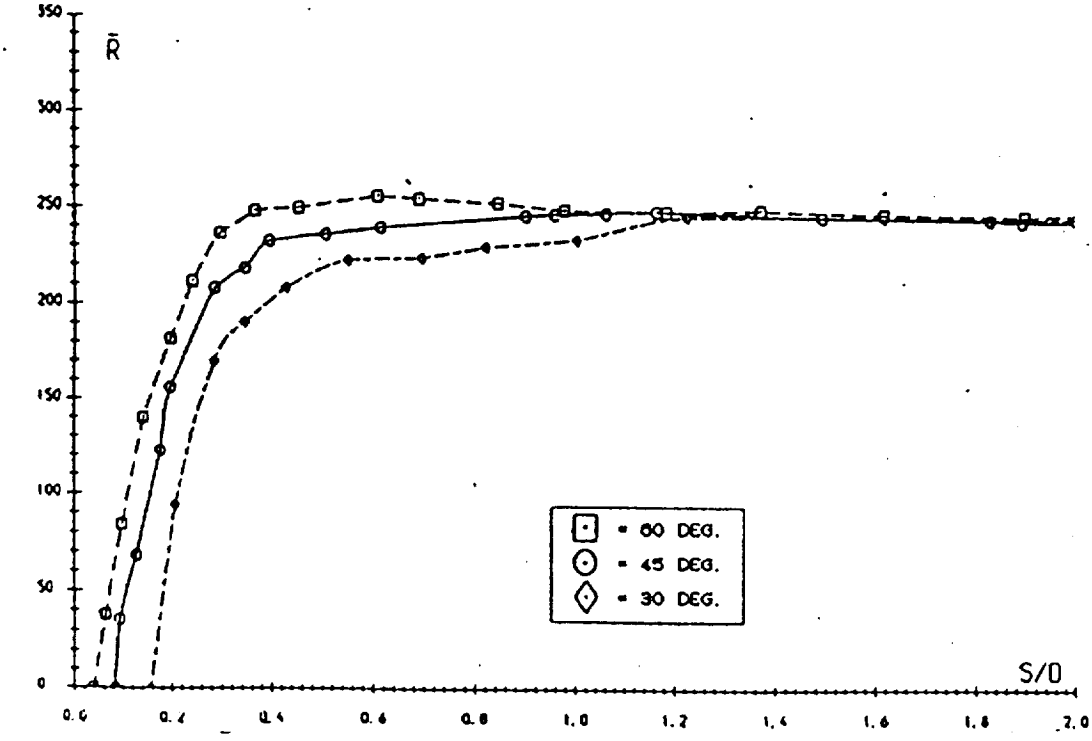

Figure 22. Variation of $\overline{R}$ in the Wing-Fuselage Junction, From Bergin

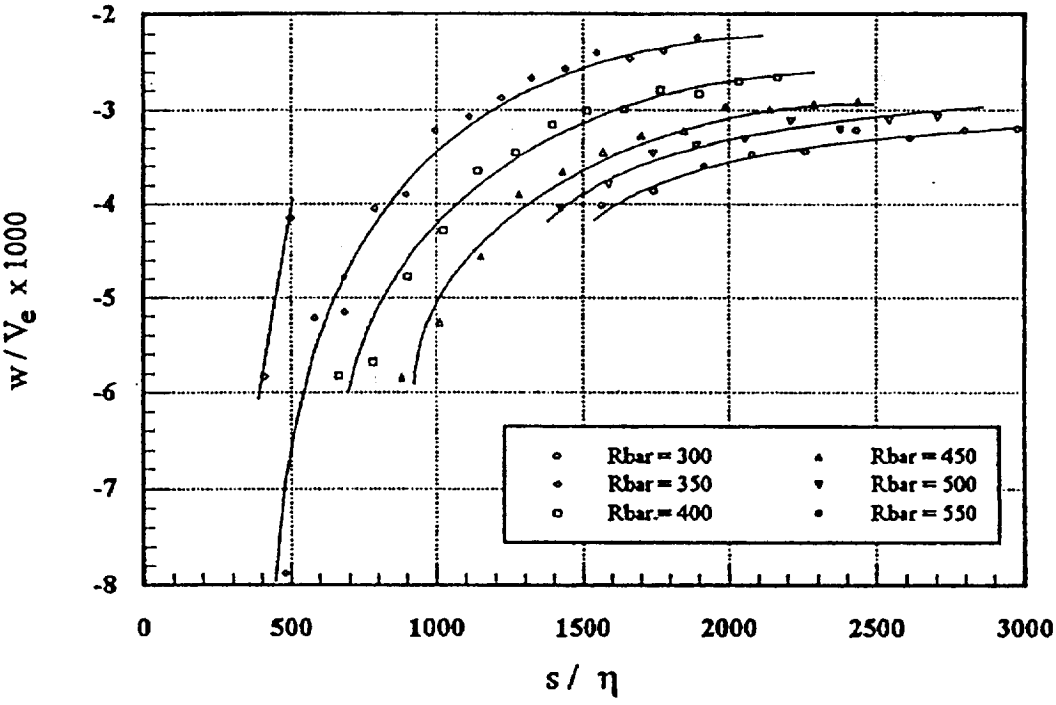

Figure 23. Critical Suction Rate For the End of Relaminarisation, From Danks and Poll

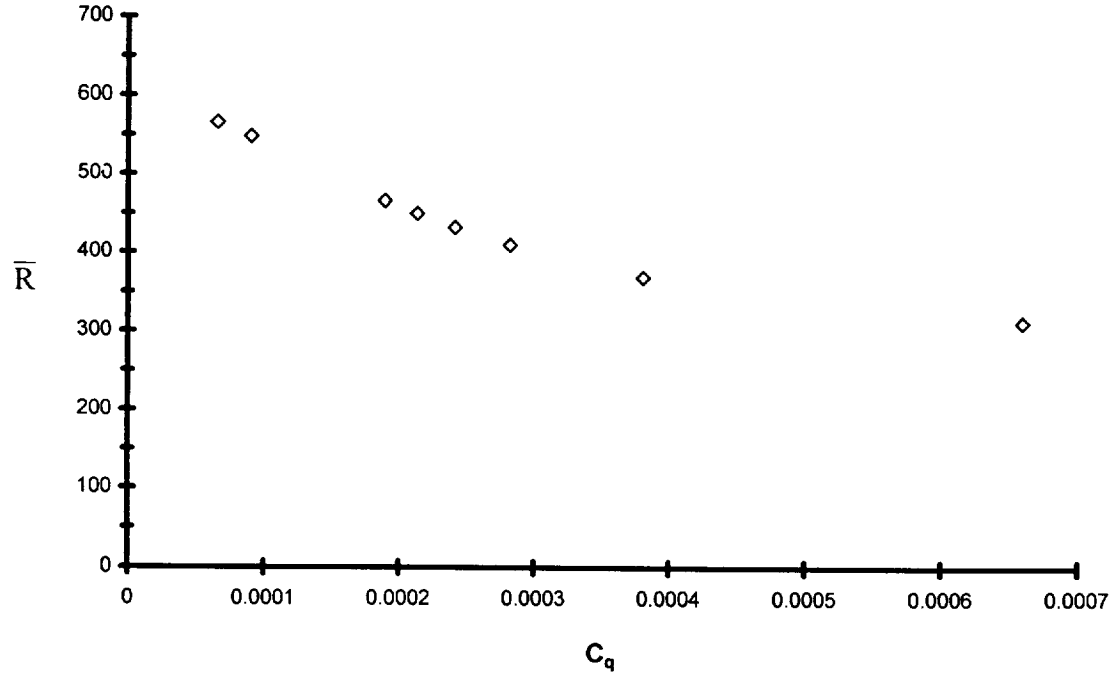

Figure 24. Attachment-Line Transition Characteristics Caused by Blowing

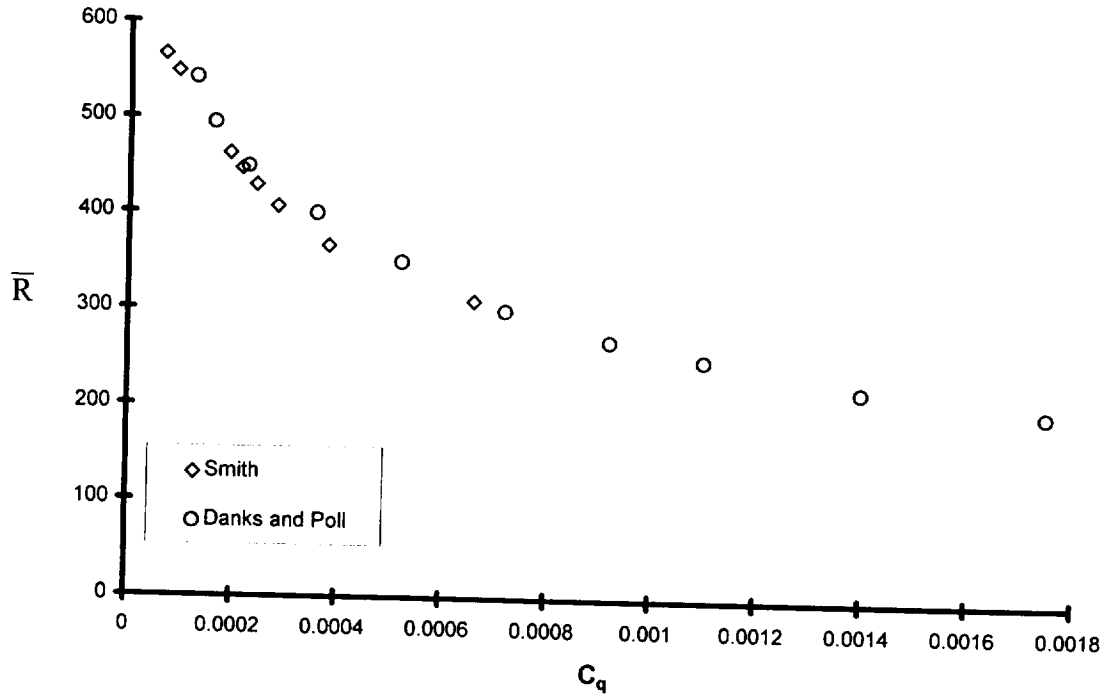

Figure 25. Comparison of Attachment-Line Transition Characteristics Caused by Blowing With Danks and Poll

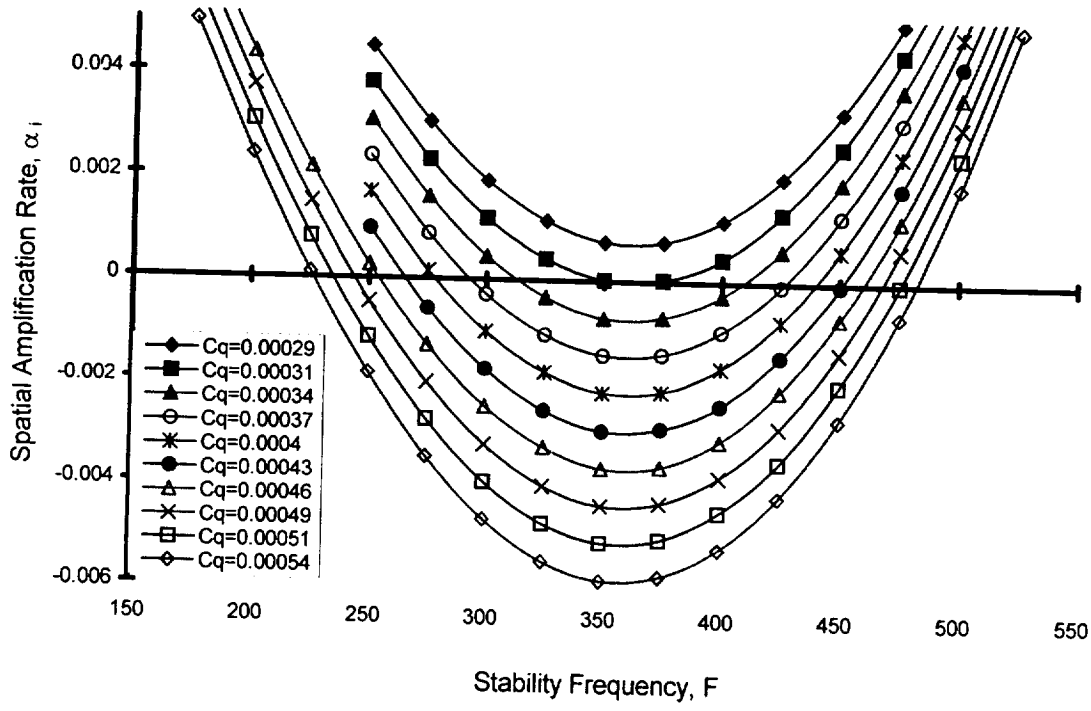

Figure 26. Linear Stability Envelope For $\overline{R}$ =350

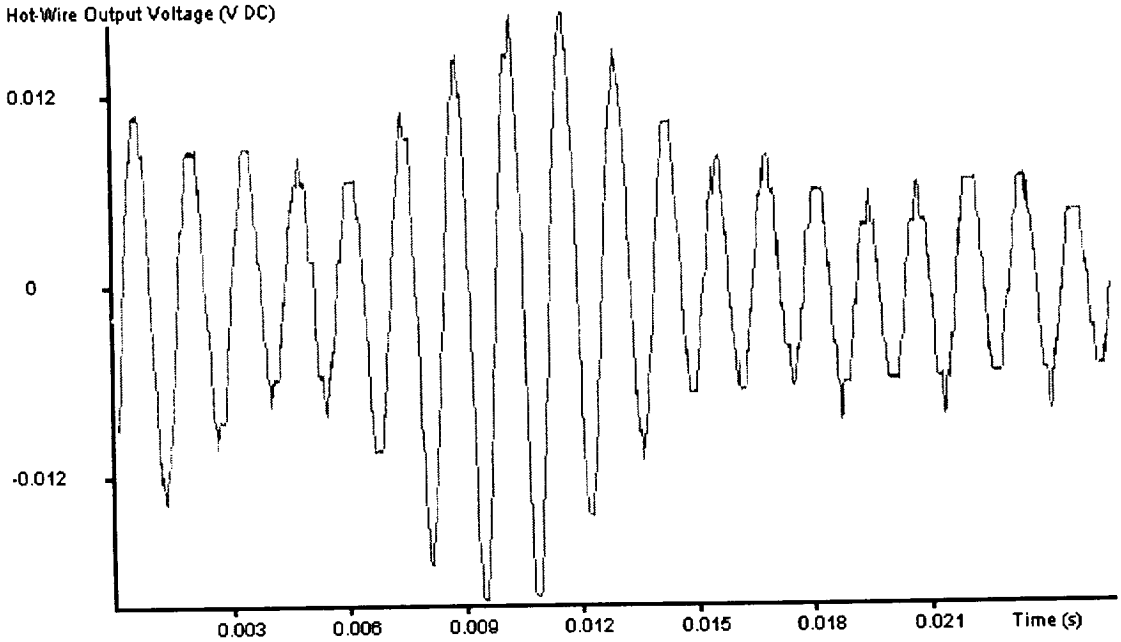

Figure 27. Example of Laminar Disturbance in an Attachment-Line With Blowing; $\overline{R}$ =372, C_q=0.000349, s/η=1900

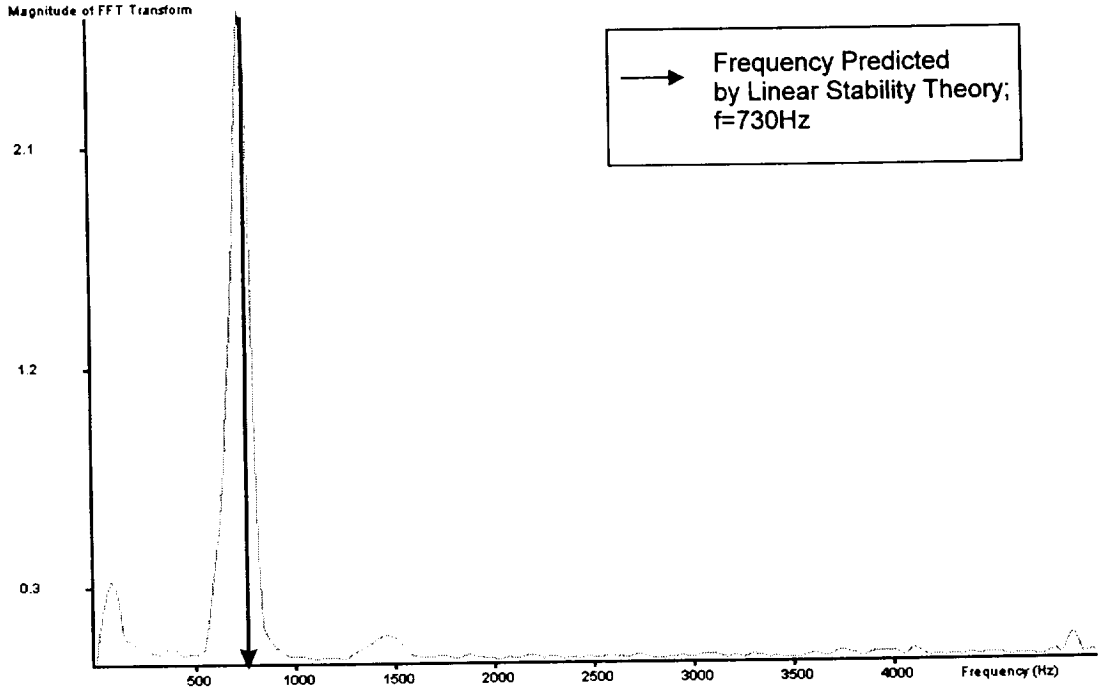

Figure 28. Amplitude Spectrum of Laminar Disturbance; $\overline{R}$ =372, C_q=0.000349, s/η=1900